

Pharmacokinetic/Pharmacodynamic (PK/PD) Analysis using Positron Emission Tomography (PET) for Preclinical Evaluation of E2110

著者	Nakatani Yosuke
学位授与機関	Tohoku University
学位授与番号	11301甲第15672号
URL	http://hdl.handle.net/10097/58335

博士論文

*Pharmacokinetic/Pharmacodynamic (PK/PD) Analysis using
Positron Emission Tomography (PET) for Preclinical
Evaluation of E2110*

(E2110 の前臨床評価を目的とした

PET による薬物動態学/薬力学(PK/PD)解析)

東北大学大学院医学系研究科医科学専攻
分子・神経イメージング講座
分子・神経イメージング分野

中谷 陽介

Table of Contents

<i>List of Original Publication</i>	5
<i>Summary</i>	6
<i>Background</i>	9
<i>Aims of This Study</i>	13
<i>Chapter. 1 A Pharmacokinetic/Pharmacodynamic PET Study of Central Serotonin 1A Receptor Occupancy by A Potential Therapeutic Agent for Overactive Bladder ..</i>	15
<i>§ 1 Introduction</i>	15
<i>§ 2 Materials and Methods</i>	18
<i>§ 3 Results</i>	30
<i>§ 4 Discussion</i>	34
<i>Chapter. 2 PET-characterization of [¹¹C]E2110 binding to 5-HT_{1A} receptors in rat brain.</i>	40
<i>§ 1 Introduction</i>	40
<i>§ 2 Materials and Methods</i>	42
<i>§ 3 Results</i>	47
<i>§ 4 Discussion</i>	48
<i>Conclusion</i>	54
<i>References</i>	59
<i>Figures</i>	73
<i>Tables</i>	87
<i>Acknowledgements</i>	89

Abbreviations

5-HT	Serotonin
8-OH-DPAT	8-hydroxy-2-(di- <i>n</i> -propylamino)-tetralin
ANOVA	Analysis of variance
BBB	Blood-brain barrier
BCRP	Breast cancer resistant protein
BP_{ND}	Binding potential
CER	Cerebellum
CNS	Central nervous system
DRN	Dorsal raphe nucleus
E_{max}	Maximum effect
HIP	Hippocampus
IP	Intraperitoneal administration
IV	Intravenous administration
K_d	Dissociation constant
K_i	Inhibition constant
$K_{p,brain}$	Brain-to-plasma concentration ratio
MPFC	Medial prefrontal cortex

MPPF	2'-methoxyphenyl-(<i>N</i> -2'-pyridinyl)- <i>p</i> -fluorobenzamidoethylpiperazine
OAB	Overactive bladder
PD	Pharmacodynamics
PET	Positron emission tomography
P-gp	P-glycoprotein
PK	Pharmacokinetics
RO	Receptor occupancy
ROI	Region of interest
SCL	Superior colliculus lesion
SD	Sprague-Dawley or Standard deviation
SRTM	Simplified reference tissue model
WAY-100635	<i>N</i> -[2-[4-(2-methoxyphenyl)-1-piperazinyl]ethyl]- <i>N</i> -(2-pyridinyl)cyclohexanecarboxamide

List of Original Publication

This thesis is based on the following publication:

- 1. Nakatani Y. Suzuki M. Tokunaga M. Maeda J. Sakai M. Ishihara H. Yoshinaga T. Takenaka O. Zhang MR. Suhara T. Higuchi M**

A Small-animal Pharmacokinetic/Pharmacodynamic PET Study of Central Serotonin 1A Receptor Occupancy by A Potential Therapeutic Agent for Overactive Bladder.

PLoS One. 2013; 8(9): e75040.

Summary

Drug discovery and development is time consuming and a costly procedure. Considering the current high failure rate of drugs that enter clinical trials, there is a clear need for more efficient and sensitive strategies in the search for useful medicine. The challenges for the pharmaceutical industry range from the evaluation of potential new drug candidates, the determination of drug pharmacokinetics/pharmacodynamics, the measurement of biomarker response as a determinant of drug efficacy, and the pharmacological characterization of mechanisms of action. Positron emission tomography (PET) is a powerful quantitative imaging technique for looking at biochemical pathways, molecular interactions, drug pharmacokinetics and pharmacodynamics. In this thesis, I conducted the pharmacological characterization of a novel 5-HT_{1A} antagonist, 1-{1-[2-(7-Methoxy-2,2-dimethyl-4-oxochroman-8-yl)ethyl]piperidin-4-yl}-*N*-methyl-1*H*-indole-6-carboxamide fumarate (E2110) by using small-animal PET and assessed the potency of E2110 as an agent for treatment of OAB. First, PK-RO relationship of E2110 in rat was evaluated with specific tracer [¹¹C]WAY-100635. Subsequent PK/PD modeling and simulation was performed based on the obtained data to investigate RO data could be a useful pharmacological indices for understanding pharmacological efficacy in animal model. Moreover, the drug-target

interaction was investigated more directly using radiolabeled E2110 ($[^{11}\text{C}]\text{E2110}$) by *in vivo* Scatchard analysis.

Central 5-HT_{1A} receptor occupancy was evaluated at different oral doses of E2110 and time points after treatment in rats. Time-radioactivity curves after administration of $[^{11}\text{C}]\text{WAY-100635}$ were analyzed by simplified reference tissue model (SRTM) and binding potential based on specific binding compared to nondisplaceable uptake (BP_{ND}) were estimated. Obtained occupancy data were analyzed by “static” (simple E_{max} model) or “dynamic” (effect compartment model with plasma pharmacokinetic profile of E2110) approach. The plasma concentrations inducing 50% RO (EC_{50}) estimated were in good agreement in both models. Also, the EC_{50} values did not markedly differ between MPFC and DRN. These findings indicate that E2110 has equal antagonist activities against pre- and post-synaptic 5-HT_{1A} receptors. Meanwhile, these *in vivo* EC_{50} values were supposed to be comparable to the *in vitro* K_i value (0.045 nM) take into account the free fraction in plasma and P-gp susceptibility of E2110. The estimated parameters were used to simulate RO profile in pharmacological model. Dose-dependent therapeutic effects of E2110 on dysregulated micturition in different rat models of pollakiuria were also consistently explained by achievement of 5-HT_{1A} RO by E2110 in a certain range ($\geq 60\%$). These findings support the possibility of PET RO

as a surrogate biomarker to evaluate the drug acting on 5-HT_{1A} receptors and associate it with counteracting effect of E2110 on OAB.

In addition, direct ligand-target interaction was investigated by using radiolabeled E2110. *In vivo* Scatchard analysis was performed under the transient equilibrium condition of specific binding of E2110. Under the condition that P-gp activity on BBB was intentionally inhibited by pretreatment of potent P-gp inhibitor, elacridar, the affinity of E2110 to the central 5-HT_{1A} receptor was investigated. The regional differences of expression level of P-gp might affect to the estimation of binding affinity of E2110, the supposed free-based K_d value was close to that obtained by *in vitro* receptor binding assay.

In summary, the use of PET in early drug discovery could provide the pharmacological information about the relationship between *in vitro* and *in vivo* for novel CNS drugs. Further PK/PD modeling and simulation approach using PET could be a powerful translational tool to bridge the gap between drug discovery in animals and drug development in human patient.

Background

Increasing costs of drug development and reduced pipeline productivity have been growing concerns for new drug development in recent years. It has been estimated that the total discovery costs of a new medicine to the completion of phase 3 clinical trials can now take up to 15 years and cost up to \$1.5BN^[1]. In spite of that, historically, only 14% of the tested products entering Phase 1 trials eventually cleared the hurdle of gaining approval and entered the market. More than 50% of this attrition resulted from failure to demonstrate efficacy in phase 2 studies^[2]. In particular, the success rate of drugs targeting disorders of the central nervous system (CNS) is half of the overall clinical approval success rate and the mean clinical-plus-approval phase time for U.S.-approved CNS drugs was 32 months or 35% longer than that for non-CNS drugs^[3]. As a consequence, despite there is a significant unmet medical need for therapeutics, several pharmaceutical industries have decreased their investments for CNS drug discovery and development^[4].

Many of these failures occur due to the lack of bridging activities in preclinical stage. To reduce the risk of failure caused by insufficient information about drug action and target molecule, the activities which bridge the gap between drug discovery in animals and drug development in human patients are required as translational research.

Translational research activities in pharmaceutical industry aim to predict the biomarker profiles or pharmacological effects in clinical situations based on *in vitro* or preclinical information. To conduct the translational drug research, understanding and learning the physiology and the mechanisms involved in drug distribution and drug-target interaction processes at a preclinical level are helpful to scale those processes to human^[5].

One of the most established approach in translational research is molecular imaging using Positron Emission Tomography (PET)^[6]. PET is a non-invasive molecular imaging technique which provides functional information of physiological, biochemical and pharmacological processes in laboratory animals and humans^[7-10]. Quantitative information from PET analysis enables us to monitor the change of target function by drug treatment. Over the last fifteen years, the importance of imaging as a critical tool for drug development has been recognized. This has been enhanced by technological advances in the realm of small animal imaging that have demonstrated their potential as translational tools^[11,12]. Currently, molecular imaging is an essential tool for translational research and new drug development.

Additionally, in recent years, pharmacokinetic/pharmacodynamic (PK/PD) modeling approaches in translational drug research are increasingly used to understand the relationship between drug concentration profiles and drug effects/target marker

profiles^[13]. This methodology is applied in drug discovery and development areas such as the selection of drug candidates with the most favorable PK/PD properties and the prediction of exposure response in patients with the aim of optimizing the design of early clinical trials. The modeling of PK/PD relationships can be of great value in understanding drug action and finding a drug dosing regimen that results in optimal therapeutic outcome^[14-18]. The use of PK/PD modeling relies on the prediction of the time course of drug action in patients using nonclinical information, because nonclinical studies are useful alternatives for investigating PK/PD relationships to get insight into the *in vivo* mechanism of drug action. The integration of PK/PD modeling and simulation has provided valuable opportunities for accelerating the evaluation of new chemical entities in the clinic and can in principle contribute to shortening the overall period of drug development process. Due to the extraordinary time and cost of drug development, it is highly desirable for pharmaceutical industries to have effective tools to confirm the action of selected compound for targets and target engagement for therapeutic indications.

1-{1-[2-(7-Methoxy-2,2-dimethyl-4-oxochroman-8-yl)ethyl]piperidin-4-yl}-*N*-methyl-1*H*-indole-6-carboxamide fumarate (E2110) is a novel compound with high selectivity and affinity to 5-HT_{1A} receptors. In control of lower urinary tract function,

many pharmacological studies in animals have revealed that 5-HT receptor agonists or antagonists modulate reflex bladder and urethral sphincter activity^[19-23]. Among them, it has been reported that 5-HT_{1A} receptor antagonist is expected to improve symptoms associated with overactive bladder (OAB)^[24, 25].

This thesis highlights the significance of *in vivo* proof-of-target/mechanism/efficacy studies to evaluate the potential of antagonist of 5-HT_{1A} receptors to treat OAB. This PK/PD framework using small-animal PET would help to scale information from *in vitro* binding studies and preclinical receptor occupancy studies to predict human 5-HT_{1A} RO and pharmacological efficacy.

Aims of This Study

The purpose of this thesis study was to evaluate the utility of quantitative molecular imaging (e.g., receptor occupancy, *in vivo* receptor binding assay) using small-animal positron emission tomography for CNS drug discovery and development as a biomarker and to develop a translational pharmacokinetic and pharmacodynamic (PK/PD) modeling framework by integrating *in vitro*, and *in vivo* preclinical data with PK/PD models to predict the effects of drugs in humans. For this aim, occupancy of 5-HT_{1A} receptor by E2110 was quantified in living rat brains by a high-resolution PET system with a radioligand suitable for imaging of the target molecule. The obtained pharmacodynamic data were fitted by the pharmacokinetic data of E2110 with mathematical model. The constructed PK/PD (RO) model for E2110 was used as the tools to predict the target receptor occupancy of E2110 for the preclinical model for OAB. The *in vitro-in vivo* correlation of pharmacological activity of E2110 were discussed by both PK-RO relationship and *in vivo* Scatchard analysis using radiolabeled E2110. In accordance with the results of modeling and simulation of 5-HT_{1A} receptor occupancy and pharmacological efficacy in animals, the required target occupancy level for the pharmacological effect was discussed.

In the Chapter 1, the RO-plasma concentration profile and RO-time profile after

oral administration of E2110 to rats were investigated with [¹¹C]WAY-100635, a specific radioligand for 5-HT_{1A} receptor. Based on the results of PK-RO analysis, RO profiles in animal pharmacological model were projected. Pharmacological effect of E2110 on micturition in different rat models of pollakiuria was explained by the range of 5-HT_{1A} RO achieved by E2110.

In the Chapter 2, distribution and binding affinity in different brain regions were examined by means of PET with [¹¹C]E2110. For the improvement of brain entry of [¹¹C]E2110, elacridar was pretreated as P-gp inhibitor at BBB. Under this condition, various specific radioactivities of [¹¹C]E2110 were injected. *In vivo* Scatchard analysis was performed based on the specific binding data at the point when transient equilibrium was established. Estimated binding affinity data (K_d) were compared with K_i value obtained by *in vitro* receptor binding assay and EC₅₀ value in receptor occupancy study with [¹¹C]WAY-100635 in Chapter 1.

Chapter. 1

A Pharmacokinetic/Pharmacodynamic PET Study of Central Serotonin 1A Receptor Occupancy by A Potential Therapeutic Agent for Overactive Bladder

§ 1 Introduction

Overactive bladder (OAB) is a pathological condition symptomatically diagnosed based upon “a symptom developing urinary urgency with or without urge incontinence and usually developing frequent urination with no proven infection or other obvious pathological factors^[26].”, and is one of the most common diseases in the elderly. Most OAB cases are idiopathic, and anticholinergic agents are frequently used for its treatment. However, it is difficult to maintain sufficient dosage of an anticholinergic agent for expected efficacy without causing significant adverse events, such as dry mouth, gastrointestinal disorder, and urinary retention, thereby limiting its use^[27–29].

Several central nervous system (CNS) transmitter systems, including adrenaline, noradrenaline, gamma-aminobutyric acid, opioids, dopamine, and glutamate transmissions are known to be involved in micturition control. Serotonin (5-HT) and its

receptors may also play an important role in the regulation of micturition reflex (Figure 1). Pharmacological studies suggested that serotonin 1A (5-HT_{1A}) receptor stimulation by administration of its agonist, 8-hydroxy-2-(di-*n*-propylamino)-tetralin (8-OH-DPAT), decreased the volume threshold for bladder contractions and facilitated voiding. On the other hand, *N*-[2-[4-(2-methoxyphenyl)-1-piperazinyl]ethyl]-*N*-(2-pyridinyl)cyclohexanecarboxamide (WAY-100635), a silent 5-HT_{1A} receptor antagonist, increased residual bladder volume and thus markedly reduced voiding efficiency^[30]. Compounds with higher selectivity for 5-HT_{1A} receptors may therefore provide a significant option for the treatment of OAB.

1-{1-[2-(7-Methoxy-2,2-dimethyl-4-oxochroman-8-yl)ethyl]piperidin-4-yl}-*N*-methyl-1*H*-indole-6-carboxamide fumarate (E2110; Figure 2) is a novel compound with high selectivity and affinity for 5-HT_{1A} receptors in the rodent brain *in vitro*. [³⁵S]guanosine-5'-O-(3-thio)-triphosphate (GTP γ S) binding studies have demonstrated that E2110 is a full antagonist of 5-HT_{1A} receptors.

As the occupancy of target receptors by a therapeutic agent is intimately correlated with the intensity of its pharmacological effects, measurements of receptor occupancy (RO) may offer an objective index for assessing pharmacokinetics (PK) and pharmacodynamics (PD) of such a drug or drug candidate. Positron emission

tomography (PET) has been recognized as an important tool in drug development, since it is capable of providing valuable information on PK, BBB penetration, and PD of a receptor ligand, as exemplified by RO, in living brains of diverse species including rodents and humans. Translation of target RO data from preclinical species to humans may be a viable strategy for predicting clinical efficacy and optimal dosage of a novel therapeutic agent, given that the relationship between RO and clinical effects has been established.

This approach relies upon an understanding of the relationship between drug concentrations in plasma and CNS that results in a specific level of target occupancy. A PK/PD modeling approach has also been used to describe the relationship between drug concentrations and RO. A maximum effect (E_{\max}) model to describe this relationship was typically applied to the PD assay, but such “static” approach could be of insufficient accuracy, particularly in case of distribution of the drug from plasma to brain or binding kinetics of the drug at the receptor being relatively slow. An optimal assessment requires determination of RO and plasma concentration at multiple time points postdose. Indirect or effect compartment models may be more appropriate than direct models to describe the relationship between occupancy and plasma concentration in treatment with a drug with delayed BBB penetration and/or target PD^[31].

In the present study, I examined the utility of 5-HT_{1A} receptor PET imaging for obtaining a surrogate marker for assessing therapeutic effects of E2110 on urinary bladder dysfunctions. Occupancy of central 5-HT_{1A} receptors by E2110 was determined in rats using PET with a radiotracer, [¹¹C]WAY-100635. A compartmental PK/PD modeling approach was then utilized to describe the relationship between plasma concentration of E2110 and 5-HT_{1A} RO by E2110 in several regions of rat brains at different time points after its oral administration. The results have supported the preclinical use of PET in combination with analytical models to predict PK/PD of a drug in humans.

§ 2 Materials and Methods

Animals

The research protocols of the present work were approved by the Animal Ethics Committee of the National Institute of Radiological Sciences and the Animal Ethics Committee of Eisai Co., Ltd. and were performed in accordance with the Principles of Laboratory Animal Care (NIH publication No. 85-23, revised 1985).

Male and female Sprague-Dawley (SD) rats were purchased from Japan SLC (Hamamatsu, Japan) and Charles River Japan Inc. (Kanagawa, Japan). All rats were

kept in animal rooms maintained at 20–26°C and illuminated from 7 am to 7 pm daily, with *ad libitum* access to food and water.

Reagents

E2110 was synthesized at Eisai Co., Ltd. (Japan). WAY-100635 maleate, 5-HT and 8-OH-DPAT were from Sigma-Aldrich (St. Louis, MO, USA). [³H]2'-methoxyphenyl-(*N*-2'-pyridinyl)-*p*-fluoro-benzamidoethyipiperazine ([³H]MPPF) was from PerkinElmer Life & Analytical Sciences (Boston, MA, USA). Tamsulosin hydrochloride was purchased from WAKO Pure Chemical Industries (Osaka, Japan). All other reagents and chemicals were of analytical grade, and were commercially available.

Binding assay in rat hippocampal membrane fraction

Rat hippocampal samples were weighed, homogenized in 10-fold volume of 50 mM Tris-HCl (pH 7.4) on an ice bath, and centrifuged (50,000×g, 4°C, 20 min). The precipitate was further homogenized in a 10-fold volume of 50 mM Tris-HCl (pH 7.4) on an ice bath and centrifuged (50,000×g, 4°C, 20 min). The obtained precipitate was homogenized in 50 mM Tris-HCl (pH 7.4) to render a concentration of 100 mg tissue eq./mL. The obtained microsomal fraction was stored as a receptor stock solution at

-80°C until use. In saturation binding experiments, the suspension of hippocampal membranes (5 mg tissue eq./tube) in the tube was incubated with different concentrations (0.03–7.77 nM) of [³H]MPPF in a total 1 mL reaction volume at 25°C for 60 min. The reaction was terminated, and bound radioactivity was separated from free radioligands by filtering and washing three times with 3 mL of 50 mM Tris-HCl (pH 7.4). The radioactivity content of the filters in 5 mL of liquid scintillator (Atomlight; PerkinElmer) was counted by TR2500 scintillation counter (PerkinElmer Life & Analytical Sciences). The specific binding was determined as the difference between total and nonspecific binding, measured in the absence and presence of 100 μM 5-HT. Data were analyzed by Scatchard plot to estimate equilibrium constant (K_d) values. For the competition experiments, binding assays were carried out using 0.3 nM [³H]MPPF in the presence of various concentrations of E2110 (0.01 to 10 nM) or WAY-100635 (0.03 to 30 nM). The IC₅₀ values for E2110 and WAY-100635 were corrected to the K_i values using the K_d values of [³H]MPPF according to the following equation:

$$K_i = \frac{IC_{50}}{1 + \frac{[radioligand]}{K_d}} \quad (1)$$

where [radioligand] means the concentration of the radioligand used.

Protein binding of E2110 in rat plasma

The *in vitro* unbound fraction of E2110 in male SD rat plasma was quantified by equilibrium dialysis. One mL of the E2110 spiked sample (100, 1000 and 10000 ng/mL) and phosphate buffered saline (PBS) were applied to one and the other chambers of a dialysis cell, respectively. The cartridge was incubated in a water bath for 24 hr at 37°C. After incubation, aliquots were sampled from both chambers and submitted to determination of the concentration of E2110 in each matrix by liquid chromatography-tandem mass spectrometry. Unbound fractions for each compound were calculated as the ratio of E2110 concentration from the PBS side to that from the plasma side of the dialysis apparatus.

Radioligand synthesis

[¹¹C]WAY-100635 was prepared by ¹¹C-acylation of WAY-100634 with [¹¹C]cyclohexanecarbonyl chloride as previously described in detail ^[32]. Semi-preparative reverse-phase HPLC was used for the purification of [¹¹C]WAY-100635. Radiochemical purity of the radioligand was more than 95%. Average specific radioactivity of [¹¹C]WAY-100635 was 196.4 ± 83.4 GBq/mmol at the end of synthesis (EOS). All injections of [¹¹C]WAY-100635 were given within 30 min after EOS.

PET data acquisition

All PET scans for rats were performed with a small animal-dedicated microPET FOCUS 220 system (Siemens Medical Solutions USA, Knoxville, TN, USA), which yields a 25.8 cm (transaxial) \times 7.6 cm (axial) field of view (FOV) and a spatial resolution of 1.3 mm full width at half maximum at the center of FOV^[33]. The rats were anesthetized with 1.5–2% isoflurane in air (flow rate: 2 L/min). Their body temperature was controlled using homeothermic controller and plate with a rectal probe, and their heart rates and arterial oxygen saturations were continuously measured by a pulse oximeter (CANL-425SVA; Med Associates, St. Albans, VT, USA). Respiration rates of these animals were also monitored with a custom-made monitoring system (Nagano Electronics, Hitachinaka, Japan). A 20 min transmission scan for attenuation correction was performed using a spiraling ^{68}Ge – ^{68}Ga point source. Subsequently, list-mode scans were carried out for 90 min. All list-mode data were sorted and Fourier rebinned into two-dimensional sinograms (frames: 4 \times 1, 8 \times 2, and 14 \times 5 min). Images were thereafter reconstructed using two-dimensional filtered back-projection with a 0.5 mm Hanning filter. [^{11}C]WAY-100635 was injected via the tail vein as a single bolus at the start of emission scanning. The injected dose of the radiotracer was 85.3 ± 28.6 MBq/rat (mean \pm SD).

PET data analysis

Anatomical regions of interest (ROIs) were placed on the medial prefrontal cortex (MPFC) and dorsal raphe nucleus (DRN) using PMOD[®] image software (PMOD Group, Zurich, Switzerland) with reference to the MRI template. Radioligand binding was examined by calculating the binding potential (BP_{ND} ; ratio at equilibrium of specifically-bound radioligand to that of nondisplaceable radioligand in tissue) based on a simplified reference tissue model (SRTM)^[34] using the cerebellar time-radioactivity curve as reference. Occupancy of 5-HT_{1A} receptors by E2110 was calculated using the following equation:

$$RO = \frac{BP_{ND, baseline} - BP_{ND, drug}}{BP_{ND, baseline}} \quad (2)$$

where $BP_{ND, baseline}$ and $BP_{ND, drug}$ are estimated BP_{ND} at baseline and following drug administration, respectively.

Rat RO study

To examine the dose-RO relationship at a single time point, four male SD rats, which had undergone a baseline PET imaging in advance, were scanned with PET at 4 hours after being pretreated with 4 oral doses (0.3, 1, 3, 10 mg/kg) of E2110. In this assay, approximately 250 μ L of blood samples were collected from the tail vein upon

initiation of the scan for quantification of plasma concentration of E2110. Furthermore, RO at different time points after the drug administration was examined by conducting PET scans of four male SD rats at 2, 4, 6 or 8 hours after pretreatment with a single oral dose of 1 mg/kg E2110. In addition to this series of PET assays for male rats, pilot PET scans for female rats (n = 3) were carried out at baseline and 4 hours after oral administration of 0.1 mg/kg E2110 to examine whether relationships between plasma concentration of E2110 and RO by this drug in the brain are consistent between two genders. In all experiments, scans for the same individual receiving E2110 were conducted more than 1 week apart.

PK study in rats

E2110 was administered orally to male and female SD rats, (4 animals/sex) at a dose of 1 mg/kg. Blood samples were collected from the jugular veins by heparinized syringes at 0.25, 0.5, 1, 2, 4, 6, and 8 hours after dosing.

Quantitative bioanalysis.

Concentrations of E2110 were determined in plasma or PBS by liquid chromatography-tandem mass spectrometry. Samples (5 µL) were injected into an L-

column ODS (35 × 2.1 mm; 5 μm, Chemical Evaluation and Research Institute, Tokyo, Japan) with a flow rate of 0.6 mL/min. 0.1% formic acid in water and acetonitrile were used as mobile phase A and B, respectively. The gradient elution started with a gradient from 0% to 100% mobile phase B for 2 min, then 1 min of 100% B, followed by a gradient of 100% to 0% for 0.01 min at the end, at a flow rate of 0.6 mL/min. The mass spectrometer (Quattro Ultima-Pt; Micromass, Waters Ltd., Manchester, UK) was operated in a positive ion multiple reaction monitoring mode. E2110 was monitored using mass transitions of 490.4/459.2. Tamsulosin was used as an internal standard, and was monitored using a mass transition of 409.3/200.0. The lower limit of quantification of E2110 in plasma was 0.5 ng/mL.

PK/PD modeling

1) Analysis of dose-RO relationships

As described in previous studies on 5-HT_{1A} receptor antagonists^[35–37] the relationship between RO and plasma drug concentration at equilibrium can be described according to the law of mass action by the curvilinear function, based on the assumption that the free brain concentration is equal to free plasma concentration and the free fraction in plasma is not concentration-dependent:

$$RO(\%) = \frac{RO_{max}}{K_d^{app} + C_p} C_p \quad (3)$$

where RO_{max} is the maximum occupancy that can be induced by E2110, K_d^{app} the apparent equilibrium constant, and C_p the plasma concentration of E2110. This model is analogous to the E_{max} model:

$$E = \frac{E_{max}}{EC_{50} + C_p} C_p \quad (4)$$

where E_{max} (RO_{max}) is the maximum effect (maximum RO) and EC_{50} ($= K_d$) is the E2110 plasma concentration required to produce 50% of E_{max} . EC_{50} can be converted to “free” based EC_{50} by multiplying the unbound fraction ratio in plasma. In this study, the relationship between E2110 plasma concentration and RO was characterized by fitting the E_{max} model to the experimental data.

2) Time-course study

The effect compartment model is illustrated in Figure 3. The mean plasma concentration profile of E2110 in each of four rats was fitted by two-compartment model with first order absorption and elimination. A sigmoid E_{max} model (Equation 4) based on the concentration in the effect compartment was fitted to the PD (RO) data. PK and PD models were linked using an effect compartment model^[38] described by the following equation:

$$\frac{dC_e}{dt} = k_{e0}(C_p - C_e) \quad (5)$$

where C_p and C_e are concentrations of E2110 in the plasma and effect compartments, respectively, and k_{e0} represents the equilibration rate constant for the effect compartment. PK and PD parameters were estimated by using SCIENTIST (Version 2.01, MicroMath Research, UT, USA).

Pharmacological tests

Female SD rats were used for pharmacological assays to assess effects of E2110 on micturition functions, since insertion of a urinary catheter into the bladder could be readily performed in female rats.

1) 5-HT_{1A} receptor agonist-induced model of OAB

Catheter implantations and cystometric investigations were performed based on the reported method^[39]. Briefly, on the day before the cystometric experiment, female SD rats were initially anesthetized with pentobarbital (50 mg/kg, IP). Catheters were inserted into the femoral vein, the dome of the stomach and the dome of the bladder. In the cystometric study, the bladder catheter was connected to an infusion pump and a pressure transducer (DX-312; Nihon Kohden Co., Tokyo, Japan) by three-way stopcock.

Saline was infused into the bladder and femoral vein. After bladder pressure was stabilized, 8-OH-DPAT (0.06 mg/kg/hr) was infused into the femoral vein instead of saline. Bladder pressure was monitored with a pressure transducer and a pressure amplifier (AP-601G; Nihon Kohden), and recorded on a pen recorder (WT-645G; Nihon Kohden). The following three micturition intervals (i.e., intervals between consecutive peaks of bladder pressure induced at the time of bladder content evacuation) were obtained: (1) basal micturition interval (intervals before 8-OH-DPAT administration), (2) pre-administration micturition interval, (intervals immediately before administration of E2110 or vehicle), and (3) post-administration micturition interval (intervals observed between 1 and 2 hr after administration of E2110 or vehicle). The change in the micturition interval after E2110 administration was used as an index of the efficacy of the treatment. E2110 (0.03, 0.1 or 0.3 mg/kg) or vehicle was administered to four groups of eight conscious rats orally.

2) Superior colliculus lesion (SCL) model

For lesioning of the brain to stimulate the micturition reflex, anesthesia was induced in female SD rats with 4% halothane and an N₂O/O₂ (2:1) gas mixture, it was maintained with 2% halothane, and each animal was mounted onto a stereotaxic

apparatus. The skull was then exposed, and holes were drilled for the superior collicular placement (anterior = + 2.0 mm; lateral = ± 1.7 mm; horizontal = 0.0 mm) of a lesion electrode (TM-type tip; 0.7 mm \times 1.5 mm). The bilateral superior colliculi were lesioned by electrical heating at 65°C for 4 min with a lesion generator (RFG-4; Muromachi Kikai Co., Ltd., Tokyo, Japan). Catheter implantations and cystometric investigations were performed with the same methodologies as in the 5-HT_{1A} receptor agonist-induced model. E2110 (0.1, 0.3 or 1 mg/kg) or vehicle was administered to four groups of eight conscious rats orally. The three micturition intervals were obtained and drug-induced changes in the micturition intervals were evaluated. In this assay, the post-administration micturition interval was defined as the average of the micturition intervals over an observation period between 0.5 and 1 hr after administration.

Data presentation and statistical analysis

Data are expressed as mean \pm standard error of mean (S.E.M). In the pharmacological study, the statistical significance of differences between the vehicle- and E2110-treated groups was tested using one-way analysis of variance (ANOVA) followed by Dunnett's multiple comparison test. A probability (p) value of < 0.05 (two-sided) was considered statistically significant. All statistical analyses were performed

using the SAS software package version 8.1 or 8.2 (SAS Institute Japan Ltd., Tokyo, Japan).

§ 3 Results

Binding assay in rat hippocampal microsomal fraction

The affinity of E2110 for rat 5-HT_{1A} receptors was examined in brain tissues. [³H]MPPF bound to membrane preparations from the rat hippocampus with a K_d value of 0.92 nM. E2110 and WAY-100635 inhibited this [³H]MPPF binding in a concentration-dependent manner (Figure 4). K_i values of E2110 and WAY-100635 for rat 5-HT_{1A} receptor were 0.045 nM (Table 1) and 0.121 nM, respectively.

5-HT_{1A} RO studies

As MPFC and DRN represent brain areas enriched with post- and pre-synaptic 5-HT_{1A} receptors, respectively, ROIs were defined in these areas for subsequent analyses. As visually demonstrated by inhibition of [¹¹C]WAY-100635 binding in representative PET images (Figure 5), E2110 dose-dependently induced 5-HT_{1A} RO at single oral doses of 0.3, 1, 3, and 10 mg/kg in each region. The relationship between the plasma concentration of E2110 and its occupancy of 5-HT_{1A} receptors could be

described by hyperbolic function (Equation 4, Figure 6). Since high doses of E2110 (3 and 10 mg/kg) induced full occupancy of 5-HT_{1A} receptors in both ROIs, E_{max} (RO_{max}) was fixed at 100%. By applying this E_{max} model, the E2110 plasma concentration required for 50% RO (EC₅₀) was estimated to be 3.68 ng/mL (7.51 nM) and 2.64 ng/mL (5.40 nM) in MPFC and DRN, respectively (Table 1).

Protein binding and PK in rat plasma

The binding of E2110 to plasma proteins was not dependent on its concentration. The average percentage of protein-unbound E2110 in plasma was 6%. Male and female SD rats were given a single oral dose of E2110 (1 mg/kg). The time course of mean plasma concentrations was reasonably well described by a two-compartment model with first-order absorption, as displayed in Figure 7. E2110 was rapidly absorbed following oral administration, with peak concentrations in plasma (C_{max}) occurring within 1 hour after dosing in all groups of rats. Elimination of the drug from plasma occurred more slowly in females than in males.

The PK parameters for E2110 derived from these data, consisting of half-life in plasma (t_{1/2}), maximum concentration (C_{max}), time at maximum concentration (T_{max}), and area under the curve in the time course of plasma drug concentration from 0 to 8

hours after oral administration (AUC_{0-8hr}), are summarized in Table 2.

PK/PD modeling and simulation

In addition to the plasma concentration of E2110, its occupancy of 5-HT_{1A} receptors (Figure 8A) was monitored in four male SD rats over the time course of 8 hours after a single oral dosing (1 mg/kg). The two-compartment model with first-order absorption fitted to the temporal profile of the mean plasma concentration of E2110 was then linked to an effect compartment sigmoidal E_{max} model (Figure 3). The peaking (1.5 hr) and subsequent decline of 5-HT_{1A} RO by E2110 were somewhat retarded relative to the plasma kinetics (Figure 8A), and this slight delay was also indicated by the hysteresis curve (Figure 8B). Estimated PD parameters derived from this analysis are listed in Table 1. The EC_{50} value for occupancy of 5-HT_{1A} receptors by E2110 in MPFC and DRN were estimated to be 2.87 ng/mL (5.85 nM) and 3.61 ng/mL (7.38 nM), respectively. Despite the time lag between the plasma PK and brain RO, these values were rather close to those estimated by the direct model, indicating that there were no marked hysteresis effects. These PD parameters were utilized to simulate the 5-HT_{1A} receptor occupancy versus time profiles in female SD rats (Figure 9). In order to assess the validity of this simulation data for predicting RO by E2110, an additional PET study

in female rats was performed to determine 5-HT_{1A} RO at 4 hours after oral administration of 0.1 mg/kg of E2110, and found that RO values measured by PET were in good agreement with calculated data (Figure 9), justifying the use of simulation curves to estimate RO in female rats.

Effects of E2110 on micturition reflex in rats

The effects of E2110 on urinary function were evaluated in rats. The micturition intervals in female SD rats were markedly decreased from the basal level by intravenous infusion of 8-OH-DPAT (n = 8; Figure 10A) or SCL (n = 8; Figure 10B). Oral administration of E2110 at doses of 0.1–0.3 mg/kg in 8-OH-DPAT treatment and 0.3–1 mg/kg in the SCL model experiment significantly (p < 0.05) prolonged the micturition intervals. According to the simulation data (Figure 9), 0.1 mg/kg of E2110 induced 60–70% RO at 1–2 hours after dosing in 8-OH-DPAT treatment, and 0.3 mg/kg of E2110 resulted in 60–80% RO at 0.5–1 hour after dosing in SCL model. From this, it can be inferred that at least 60% RO is required for significant effects of E2110 on micturition.

§ 4 Discussion

In recent years, PK/PD modeling has been increasingly applied in drug discovery and early drug development. Preclinical PK/PD studies may prompt a series of important mechanistic studies to investigate the relationship between plasma concentrations and resulting effects on a biomarker in later stages of clinical drug development. The PK/PD modeling and simulation approaches to preclinical pharmacology studies may help to understand the mechanism of action of novel compounds and target engagement in preclinical models. The present data have demonstrated the utility and robustness of *in vivo* PET imaging techniques to monitor RO in living brains of small animals. Both direct and indirect models yielded a good fit to the experimental data and similar EC_{50} values for the drug under development, E2110, validating the use of these methodologies in rats and, potentially, humans. The dose-dependent effects of E2110 on bladder micturition function were consistently explained by the time course of RO induced by the drug, allowing prediction of pharmacologically efficacious doses of the drug by clinical PET estimation of RO.

Based on the results of dose-response PET study conducted at a fixed time point after E2110 treatment, 5-HT_{1A} RO was well fitted by a simple E_{max} model, and the free concentration-based EC_{50} value did not markedly differ between MPFC (0.22

ng/mL, 0.45 nM) and DRN (0.16 ng/mL, 0.32 nM). These findings indicate that E2110 has equal antagonist activities against pre- and post-synaptic 5-HT_{1A} receptors. Meanwhile, these free concentration-based EC₅₀ values were approximately 10-fold of the K_i value (0.045 nM) calculated from the *in vitro* binding assay for 5-HT_{1A} receptor. The supplemental study indicated that E2110 is a substrate for the BBB drug transporter P-glycoprotein in rodents, as the brain-to-plasma concentration ratio (K_{p,brain}) of E2110 concentration in *mdr1a/1b*-knockout mice was ten times higher than that in wild-type mice (data not shown). Therefore, the free E2110 concentration in CNS tissues is assumed to be one-tenth of its free plasma concentration. On the basis of this assumption, the *in vivo* EC₅₀ values corrected for the difference in free drug concentrations between plasma and CNS were estimated to be 0.045 and 0.032 nM in MPFC and DRN, respectively, and these values are comparable with *in vitro* K_i. This finding also supports the reliability of PET assays for anesthetized rats to quantify 5-HT_{1A} RO. Indeed, the use of isoflurane-anesthetized rats for 5-HT_{1A} RO determination was justified in a reported [¹¹C]WAY-100635-PET study, which demonstrated that *in vivo* ED₅₀ value for pindolol in the hippocampus (5.6 mg/kg) was rather close to hippocampal ED₅₀ value (8.5 mg/kg) estimated by an *ex vivo* autoradiographic measurement for unanesthetized rats^[40].

The time course of 5-HT_{1A} RO and plasma PK after a single oral dose of E2110 (1 mg/kg) offered details of the PK-RO relationships for this drug, and enabled simulation of RO in pharmacological models. This effect compartment model well described the temporal profiles of 5-HT_{1A} RO, and the EC₅₀ values based on this PK/PD modeling were estimated to be 2.87 ng/mL (5.85 nM) and 3.61 ng/mL (7.38 nM) in MPFC and DRN, respectively. Hysteresis was observed in a plot of the relationship between plasma concentration and 5-HT_{1A} RO, and this lag time is typically observed for centrally acting compounds, due to either rate-limiting BBB passage of the compounds or slow receptor on/off targets^[41]. Although such delay was observed between RO and plasma PK of E2110, the EC₅₀ values calculated with the direct and effect compartment models were nearly equivalent. Additionally, estimates of the equilibration rate constant (k_{e0}) were relatively large, indicating a rapid equilibration with the CNS biophase (CNS equilibration $t_{1/2}$ of 1.4 hours). Therefore, hysteresis effects on the target binding of E2110 were minor in the present study.

The present work also demonstrated a profound difference in plasma PK profiles of E2110 between male and female SD rats (Table 2). Overt gender differences in expression levels of enzymes involved in drug metabolisms were reported in a

previous rat study^[42], and Chovan et al. documented that substrates of human drug-metabolizing enzyme cytochrome P450 3A4 (CYP3A4) were mainly metabolized by cytochrome P450 3A1/2 and 2C11 in rats^[43], and expression levels of these enzymes in male rats are known to be higher than in female rats^[42]. In addition, the unpublished results indicated that E2110 was primarily metabolized by CYP3A4 in human liver microsomes. Taking these findings together, it was supposed that the difference in plasma PK of E2110 between male and female rats is attributable to gender difference in the levels of hepatic cytochromes responsible for metabolism of this drug. Despite these effects of gender on PK, 5-HT_{1A} RO in the female rat brain measured by PET was close to a value calculated by effect compartment model with k_{e0} determined in male rats (Figure 9), suggesting consistency of the PK-RO relationships between males and females.

These findings in pharmacological tests have provided further support to the implication of 5-HT_{1A} receptors in the control of micturition in rats^[44, 45]. Numerous rat studies have indicated that 5-HT_{1A} receptors have an excitatory physiological role in modulating micturition^[46]. Both spinal and supraspinal 5-HT_{1A} receptors constitute an efficient way to stimulate rat micturition. However, the modulation of the 5-HT_{1A} autoreceptor has been proposed to interfere with the micturition reflex^[44, 47].

Administration of 8-OH-DPAT was reported to facilitate the voiding reflex, and this effect was inhibited by the pretreatment with 5-HT_{1A} receptor antagonists such as WAY-100635 and NAD-299^[39, 48]. The inhibitory effect of E2110 on the micturition reflex observed in the present work could accordingly be attributed to its action on supraspinal 5-HT_{1A} autoreceptors. In order to correlate the degree of 5-HT_{1A} RO by E2110 yielding significant effects in pharmacological tests, I applied simulated temporal profiles of RO in DRN enriched with putative autoreceptors after oral doses of E2110 in female SD rats (0.03, 0.1, and 0.3 mg/kg). The minimum doses of E2110 exerting overt therapeutic effects on the micturition reflex in 8-OH-DPAT and SCL models were 0.1 and 0.3 mg/kg, respectively. In reference to the simulated RO values, RO at these doses were estimated to be around 60% during the micturition monitoring period (at 1–2 hours postdose in the 8-OH-DPAT model and 0.5–1 hour postdose in the SCL model), demonstrating that RO around 60% or more was necessary for a significant effect on bladder function. Thus, for humans, the dosage of a 5-HT_{1A} antagonist would need to be determined to achieve this range of RO as a requirement for therapeutic efficacies against OAB.

In summary, these data support that occupancy of central 5-HT_{1A} receptors quantified by *in vivo* PET is a useful biomarker surrogating anti-OAB effects of 5-HT_{1A}

receptor antagonists. Although micturition is supposedly regulated by diverse neurotransmitter pathways at different levels in the central and peripheral nervous systems, the assessment PK-RO relationship using brain PET data would help to determine and/or predict effective doses of these candidate drugs in rat models. Meanwhile, several factors, including species differences in the protein-unbound fraction and the presence or absence of an active metabolite of such a provisional drug, should be taken into account in consideration of homology between EC_{50} values in laboratory animals and humans. Species differences in RO and PK-RO relationship would be assessable with the aid of comparative PET assays.

Chapter. 2

PET-characterization of [¹¹C]E2110 binding to 5-HT_{1A} receptors in rat brain.

§ 1 Introduction

In the Chapter 1, it have been demonstrated that PET can evaluate the ligand-target interaction of novel CNS drugs by examination of the competition for specific radioligand binding to the target (occupancy studies). Moreover, these tools can provide an understanding of the level of receptor occupancy required for pharmacological effect. The current results support that molecular imaging approaches with using target-specific PET tracers provide the useful information about the correlation between CNS target coverage and drug pharmacokinetics.

If a suitable PET radioligand for the target exists, it would be a very powerful translational tool in preclinical research, allowing the measurement of binding characteristics of the target (K_d and B_{max}) in tissues across species as well as enabling assessment of target occupancy during the lead optimization in drug discovery process with the unlabeled compound of interest. Furthermore, such a tool can be used to correlate target occupancy of a drug candidate with preclinical efficacy and target

engagement experiments to support the proof-of-concept (POC) in preclinical stage and to estimate the effective dose selection in clinical studies. However, drugs being developed at an early stage in the drug discovery often act at totally novel molecular sites and, as such, usually there are no existing radioligands acting at these targets. Therefore, in the absence of radioligands which directly and specifically label target molecules, the use of a radiolabeled version of candidate itself would provide useful information about the target-drug interaction.

In this study, [^{11}C]E2110 was synthesized as the tracer for the central 5-HT_{1A} receptor and *in vivo* binding potential was evaluated. E2110 showed a high affinity for 5-HT_{1A} receptor in *in vitro* receptor binding study and it was also shown by *in vivo* PET study with [^{11}C]WAY-100635. Estimated affinity of E2110 to the receptor was applicable for imaging of central 5-HT_{1A} receptor as a PET tracer. However, it was concerned about the effect of the brain efflux transporter, P-gp, on the distribution of E2110 to the brain. Therefore, in this study, elacridar was used as the chemical inhibitor for P-gp to improve the brain distribution of [^{11}C]E2110. Under the condition of inhibition of P-gp by elacridar, the pharmacological characterization of E2110 was conducted by radiolabeling E2110 itself. Binding potential of [^{11}C]E2110 was calculated by the transient equilibrium method. Transient equilibrium method has been widely

used to investigate the density (B_{\max}) and affinity (K_d) of labeled compounds [49–51]. In experiments *in vivo*, the ratio of concentration bound to targets (C_B) and nondisplaceable radioligand in brain (C_N) is equal to BP when $dC_B/dt = 0$. This moment is called transient equilibrium. To avoid cumbersome arterial blood sampling, $C_N(t)$ has been approximated with the time-activity curve (TAC) from a reference tissue devoid of specific binding sites $C_{\text{REF}}(t)$ [52, 53]. The TAC for $C_B(t)$ has then been calculated as brain tissue radioactivity ($C_T(t)$) minus $C_{\text{REF}}(t)$. Although some limitations were noted the use of $C_{\text{REF}}(t)$ instead of $C_N(t)$ [53–56], this simple approach can be useful to determine for the evaluation of ligand-target interaction in early preclinical stage.

Based on the calculated binding potential by transient equilibrium method, 5-HT_{1A} receptor affinity and density of E2110 was estimated. By using a small-animal PET with [¹¹C]E2110, ligand-target interaction was directly evaluate and the utility of this methodology in the early drug discovery stage was discussed

§ 2 Materials and Methods

Reagents

E2110 was synthesized at Eisai Co., Ltd. (Japan). Elacridar (GF120918) [*N*-(4-(2-(1,2,3,4-tetrahydro-6,7-dimethoxy-2-isoquinolinyl)ethyl)phenyl)-9,10-dihydro-5-

methoxy-9-oxo-4-acridine carboxamide] was purchased from Toronto Research Chemicals (Toronto, Ontario, Canada).

Animals

The research protocols of the present work were approved by the Animal Ethics Committee of the National Institute of Radiological Sciences and were performed in accordance with the Principles of Laboratory Animal Care (NIH publication No. 85-23, revised 1985).

Male SD rats were purchased from Japan SLC (Hamamatsu, Japan). All rats were kept in animal rooms maintained at 20–26°C and illuminated from 7 am to 7 pm daily, with *ad libitum* access to food and water.

Synthesis of radiotracers

[¹¹C]CH₃I was introduced to a solution of pre-E2110-OH (1.2 mg, 2.5 μmol) and NaOH (0.5 mol/L solution, 6 μL, 3 μmol) in DMF (300 μL) at 0 °C. The reaction mixture was heated at 40 °C for 3 min and purified by HPLC (Capcell Pak C18, S-5 μm, 10 mm ID ×250 mm, Shiseido Co., Ltd., Tokyo, Japan) using the mobile phase of Acetonitrile/H₂O/Tetraethylammonium (TEA) (5/5/0.01, v/v/v) at a flow rate of 6.0

mL/min to give 1.05 GBq of [¹¹C]E2110. The t_R of [¹¹C]E2110 was 7.3 min for purification and 6.4 min for analysis on HPLC (YMC Pack Pro C18, S-5 μ m, 4.6 mm ID \times 150 mm, YMC Co., Ltd., Kyoto, Japan) using the mobile phase of Acetonitrile /H₂O/TEA (5/5/0.01, v/v/v) at a flow rate of 1.5 mL/min. The synthesis time from EOB, 28.1 min; radiochemical yield decay-corrected, 9.2 % based on [¹¹C]CO₂; radiochemical purity, > 99%; specific activity at EOS, 213 GBq/ μ mol (n = 7).

Elacridar treatment and PET scan

All PET scans for rats were performed with a small animal-dedicated microPET FOCUS 220 system (Siemens Medical Solutions USA, Knoxville, TN, USA), which yields a 25.8 cm (transaxial) \times 7.6 cm (axial) field of view (FOV) and a spatial resolution of 1.3 mm full width at half maximum at the center of FOV^[33]. A 20 min transmission scan for attenuation correction was performed using a spiraling ⁶⁸Ge–⁶⁸Ga point source. Subsequently, list-mode scans were carried out for 150 min. All list-mode data were sorted and Fourier rebinned into two-dimensional sinograms (frames: 4 \times 1, 8 \times 2, and 26 \times 5 min). Images were thereafter reconstructed using two-dimensional filtered back-projection with a 0.5 mm Hanning filter.

Elacridar, 3 mg/kg, was administered intravenously 30 minutes before tracer

injection. [¹¹C]E2110 was injected via the tail vein as a single bolus at the start of emission scanning. The injected dose of the radiotracer was 126.5 ± 10.9 MBq/rat (mean \pm SD). For the determination of densities and affinities, the tracer containing various amounts of cold mass (0, 10, 30, 60, and 600 nmol) for 5 different PET scans was used. In experiments, scans for the same individual receiving E2110 were conducted more than 1 week apart.

PET data analysis

Anatomical regions of interest (ROIs) were placed on the medial prefrontal cortex (MPFC), hippocampus (HIP) and cerebellum (CER) using PMOD[®] image software (PMOD Group, Zurich, Switzerland) with reference to the MRI template. Time-radioactivity curve of each region was expressed in %ID/mL, normalized to the injected radioactivity, and plotted against time.

In vivo Scatchard analysis

The data were obtained at systematically varied ligand concentrations and analyzed by means of Scatchard plots^[53, 57, 58]. The binding parameters for [¹¹C]E2110 were obtained by performing 5 separate scans and various specific radioactivities on one

animal. For the low specific-radioactivity conditions, 10–600 nmol of cold E2110 was added to the tracer. The hyperbolic saturation curve of tracer binding was defined as:

$$B = B_{max} \times \frac{F}{K_d + F} \quad (6)$$

In case of two-site binding, the hyperbolic equation (Equation 6) is modified to the following equation:

$$B = B_{max1} \times \frac{F}{K_{d1} + F} + B_{max2} \times \frac{F}{K_{d2} + F} \quad (7)$$

where B is the concentration of bound ligand (pmol/mL), F is the concentration of free ligand (pmol/mL), B_{max} is the total receptor density (pmol/mL), and K_d is the dissociation constant (nM). The total radioligand concentration in the cerebellum (reference region) which was used as an estimate of F, since the density of 5-HT_{1A} receptors is negligible in cerebellum. Specific binding (B) was defined as the difference in radioactivity between specific binding regions (ROIs) and reference region. Transient equilibrium is established when the radioactivity in each ROIs is maximal^[53,57] and at this timepoint, the derivative for specific binding was 0 ($dC_b/dt = 0$). The equilibrium time was defined by fitting the curve for B to a 3-exponential equation^[59]. The B_{max} and K_d values were calculated by nonlinear hyperbolic analysis with the equation one-site model (Equation 6) or two-site model (Equation 7) using the fitting software Prism (GraphPad Software, San Diego, CA, USA). Also, the regressed hyperbolic curve (x is

F and y is B) was transformed to create the Scatchard plot graph (x is B and y is B/F).

§ 3 Results

Effect of Elacridar on [¹¹C]E2110 brain distribution

The representative PET images in brain with or without elacridar treatment are shown in Figure 11. Pre-treatment of elacridar (3 mg/kg, IV) dramatically improved the brain distribution of [¹¹C]E2110. Also, high accumulation of [¹¹C]E2110 was observed in a pattern consistent with the known central 5-HT_{1A} receptor distribution [60]. Representative time-radioactivity curves of [¹¹C]E2110 in each condition are also shown in Figure 11.

In vivo Scatchard analysis by [¹¹C]E2110 PET with multidose ligand treatment

With increasing doses of unlabeled E2110, the radioactivity showed a stepwise attenuation in all regions. The dose-dependent reduction of [¹¹C]E2110 binding to 5-HT_{1A} receptor in the multidose ligand assays was observed by alterations to the time curve of specific binding in MPFC and HIP. The transient equilibrium of specific binding was reached at 70–90 min in the MPFC, 55–75 min in the HIP.

Figure 12 shows the Scatchard plots for the MPFC and HIP. Equilibrium values for specific binding (B) and free [¹¹C]E2110 concentration (F) were obtained at the point dC_B/dt was 0. Based on the shapes of Scatchard plot of [¹¹C]E2110, two-site binding model was used to fitting. The *in vivo* B_{max} and K_d values of [¹¹C]E2110 in two ROIs are summarized in Table 3.

§ 4 Discussion

The BBB prevents hydrophilic compounds from entering the CNS and is thus a major hurdle in designing drugs directed at the brain. It has been estimated that 98% of small-molecule compounds do not cross the BBB in sufficient amounts ^[61], and a lack of adequate brain exposure has contributed to a significant number of failures in the development of CNS drugs ^[62]. In CNS drug research, biodistribution study with radiolabeled compound can be useful in early preclinical stage to assess if the compound crosses the BBB and to evaluate *in vivo* affinity of the compound to the target. However, there are some difficulties in the case the compound might be a substrate of active transport systems in the BBB. The supplemental research indicated that E2110 could be a substrate of P-gp. P-gp is an adenosine triphosphate-driven efflux pump expressed at BBB. Many structurally unrelated drugs, including various

anticancer drugs, antidepressants, steroids, and HIV protease inhibitors, are substrate of P-gp and are extruded from the brain by this efflux pump^[63, 64]. For the PET tracers, it is suggested that non-substrate for brain efflux transporters (e.g., P-gp and BCRP) are one of the criteria to be met ideally by radiotracers^[65]. Based on the results of this study, in rats, the free E2110 concentration in brain tissues is assumed to be one-tenth of its free plasma concentration. In terms of the pharmacological property, E2110 showed the high binding affinity to the central 5-HT_{1A} receptors both *in vitro* receptor binding assay and *in vivo* PET RO study with [¹¹C]WAY-100635. For the estimation of *in vivo* affinity to the target molecules and investigation of the correlation to the *in vitro* assay results, receptor occupancy study with specific binding tracer is useful because this kind of study could be conducted at pharmacological active dose, and even if the test compounds might be a substrate of efflux pump in the CNS, the pharmacological efficacy would be evaluated by increasing a dose. On the other hand, in the case the evaluation of *in vivo* target affinity of compounds by radiolabeled version of compound, effect of the efflux pump at BBB would be significant on the brain distribution of compound.

In animals, it has been reported that some inhibitors for these transporters are available to increase brain distribution^[64, 66-68]. Elacridar (GF 120918) is widely used as P-gp and BCRP inhibitor^[69, 70]. In *in vitro*, elacridar inhibited P-gp mediated transport

of the P-gp substrate [³H]paclitaxel in a P-gp-overexpressing cell line with inhibition constants (K_i) of 109 nM^[71]. Preclinical studies have shown that elacridar potently inhibit P-gp function at the BBB as reflected by increased brain uptake of P-gp substrates, without displaying cytochrome P450-mediated pharmacokinetic interactions^[68, 72, 73]. It has also been shown that elacridar is increasing brain distribution of verapamil and loperamide ($ED_{50} = 1.2-2.4$ mg/kg) with no effect on metabolism and plasma protein binding^[67, 72]. Elacridar also significantly increased brain distribution of several tyrosine kinase inhibitors (TKIs)^[74-79].

In the baseline experiments (i.e., before inhibition), the radioactivity level of [¹¹C]E2110 in ROIs were rather low (Figure 11), which suggested that E2110 is efficiently kept out of brain by P-gp-mediated efflux. However, the brain distribution of [¹¹C]E2110 was dramatically improved by 3 mg/kg of elacridar pretreatment. In this condition, the specific binding to the 5-HT_{1A} receptor could be assessed by multidose ligand assays with the Scatchard analysis. In this study, B/F was estimated based on the equilibrium analysis in rat brain regions.

[¹¹C]E2110 was highly accumulated in ROIs and negligible in reference tissue.

The obtained Scatchard plot indicated two-site binding model would be suitable for

fitting. Therefore, as shown in Table 3, two different types of [¹¹C]E2110 binding parameters are estimated in each brain regions.

As shown in Table 3, K_d and B_{max} values in each region were calculated from a regression line with good correlation ($R^2 = 0.82-0.87$). In MPFC, the estimated K_d value of high-affinity sites for 5-HT_{1A} receptor was 0.5 nM. This value was about 10-fold larger than the K_i value in *in vitro* receptor binding assay. Possible consideration for this gap between *in vitro* and *in vivo* is the difference of actual ligand concentration in *in vivo* this analysis. In *in vivo* RO study, K_d value was estimated by the concentration in cerebellum as free ligand concentration. However, this value includes the nonspecifically binding fraction of E2110 to the tissue. Therefore, the use of the total cerebellar activity as an estimate of the free ligand concentration leads to an overestimation of K_d value. In the Chapter.1, the plasma protein binding of E2110 was calculated to be 94%. This result indicates E2110 would be nonspecifically bound to brain tissue and about one-tenth of E2110 concentration in reference tissue would be exist as free (unbound) form. On the basis of this assumption, the K_d value obtained from *in vivo* Scatchard analysis is almost equivalent that from *in vitro* receptor binding assay.

Elacridar pretreatment could modify the activity of P-gp at BBB, but a previous animal imaging study found some evidence for a non-uniform distribution of P-gp in rat brain. Laćan et al. quantified P-gp expression by Western blot analysis and found two times higher P-gp levels in cerebellum as compared to other brain regions (e.g. hippocampus, frontal cortex) of rats^[80]. This report suggests that the *in vivo* binding study with P-gp substrate tracer have the potential to overestimate the affinity because of the regional heterogeneity of P-gp in brain. In this case, since cerebellum was used as reference tissue, it may be considered about two-fold difference would include in the estimation of K_d values. Also in HIP, Scatchard analysis suggested E2110 bound to the receptor with high affinity ($K_d = 1.1$ nM). However, the K_d value in HIP was about two-fold higher than that in MPFC (0.5 nM). These regional differences of receptor binding affinity were also suggested in receptor occupancy study with [¹¹C]WAY-100635. Based on the results of additional analysis of E2110 RO data, the EC_{50} value of E2110 in HIP was calculated to be 16.0 nM (Figure 13). These data indicated that E2110 may have different affinity to same receptor in different brain regions. Further study would be required to explain this unique behavior of E2110 to the receptors

In present study, *in vivo* Scatchard analysis was performed for the determination of B_{max} and K_d of E2110 using PET. The equilibrium analysis with

validated reference region^[60,81,82] was useful to *in vivo* measurement for pharmacologic indices of this radioligand. Also, [¹¹C]E2110 PET data combined with elacridar administration demonstrated that P-gp inhibitor can improve brain uptake and this approach would be a useful even if the radiolabeled compound is supposed to be a P-gp substrate. Non-uniform distribution of P-gp in brain was suggested that regional activities may need to be factored into PET kinetics of tracers that are substrate for P-gp to enable accurate quantification of receptor densities in *in vivo*. In many cases, lead compounds with desirable pharmacological activity may have undesirable properties related to pharmacokinetics in early preclinical stage. Present study demonstrated that PET imaging technique provides the opportunity to obtain proof of mechanism (POM) of the compound so that later studies can be performed with the confidence that the compound is acting as expected. In addition, the investigation of *in vitro-in vivo* relationship in pharmacological activity would help the optimal estimation of effective dose in human.

Conclusion

In 2004, the Food and Drug Administration (FDA) released an article titled: “Innovation or Stagnation: Challenge and Opportunity on the Critical Path to New Medical Products.”^[83] In this article, the FDA defines biomarkers as “quantitative measures of biological effects that provide informative links between mechanism of action and clinical effectiveness” and surrogate endpoint as “quantitative measures that can predict effectiveness.” The purpose of this thesis is to evaluate the utility of quantitative molecular imaging using small-animal PET for CNS drug discovery and development as a biomarker. The interaction between central 5-HT_{1A} receptor and E2110 which is a novel antagonist of this receptor was investigated by several methodologies including receptor occupancy, PK/PD modeling, and *in vivo* Scatchard analysis. Obtained biomarker response was used to predict the pharmacological efficacy in animal models and endpoint in preclinical stage was discussed. The primary observations in the present study are summarized as follows:

- 1) The plasma concentration-dependent occupancy of central 5-HT_{1A} receptors by E2110 was demonstrated by *in vivo* PET with specific tracer [¹¹C]WAY-100635. The PET study indicated that the occupancy data would be a useful biomarker surrogating anti-OAB effects of novel 5-HT_{1A} receptor antagonists. Also, the

assessment PK-RO relationship using brain PET data would help to determine and/or predict effective doses of E2110 in animal models.

- 2) Binding parameters (K_d , B_{max}) of E2110 for rat central 5-HT_{1A} receptors were determined by using multidose ligand approach with radiolabeled E2110 (¹¹C]E2110). 3 mg/kg of elacridar treatment improved the brain uptake of E2110 and successfully conducted the *in vivo* Scatchard analysis. The binding characteristics will aid the understanding the *in vitro-in vivo* correlation of pharmacological activity of compound and exposure-efficacy relationship in animal models.

Throughout this research, the pharmacological activity of E2110 as a central 5-HT_{1A} receptor antagonist was well characterized *in vitro* and *in vivo*. As the results, the *in vitro* 5-HT_{1A} receptor affinity (K_i) of E2110 in rat was close to the parameter that was estimated from PET receptor occupancy and Scatchard analysis *in vivo*. The relationship between pharmacological efficacy and 5-HT_{1A} receptor occupancy was also assessed and was clarified as the target 5-HT_{1A} receptor occupancy over 60% in the animal model of overactive bladder. With respect to the requirement of receptor occupancy for pharmacological efficacy of CNS targeted drugs, it has been reported that 60–80% of occupancy would be required for GPCR antagonists^[84]. However, these occupancy

requirements still have to be discussed in terms of time point of occupancy assessment, and clinical relevancy of animal models and contribution of 5-HT_{1A} receptor to the control of bladder function. In terms of the side effects that are related to 5-HT_{1A} receptor blockade, Rabiner et al. evaluated the central 5-HT_{1A} receptor occupancy by novel full antagonist, DU125530^[36]. Based on the report, DU125530 displayed a dose-dependent occupancy of the 5-HT_{1A} receptor in the human brain, reaching up to 72% with minimal side effects. These reports indicate E2110 would show the efficacy with no serious side effects by optimization of therapeutic dose based on the occupancy information. Therefore, PK/PD relationship established in this study would be useful in the translational approach to estimate the E2110 dose required for anti-OAB effect in further clinical trials. Also, these preclinical findings suggest that receptor occupancy is a meaningful PD biomarker for understanding the drug-receptor interaction that underlies a pharmacological effect and is useful for predicting the effective and safe dose ranges given drug candidate. E2110 have high affinity to 5-HT_{1A} receptor and have shown pharmacological efficacy in animal model, but [¹¹C]E2110 at a tracer level could not show the distribution to the brain. This result demonstrated that the contribution of P-gp efflux to brain penetration of E2110 was critical at a tracer dose, while a significant amount of E2110 could enter in brain at effective dose. In this study, the

brain penetration of [¹¹C]E2110 was improved by pre-treatment of elacridar and *in vivo* binding parameters were successfully estimated by using small-animal PET.

In recent years, imaging techniques are widely applied in drug discovery and development for evaluation of CNS drug disposition and for validation of disease biomarkers and tracers for novel targets^[85-87]. Imaging at the molecular level provides a direct measure of mechanism of action, offering a more predictive measure of drug activity through the use of targeted image-based predictive biomarkers. As a result of these efforts, imaging is now being used to drive go/no-go decisions in early discovery, and there is a significant focus on developing and validating image-based biomarkers that are intended to be applicable for use in clinical trials. The results of this research also support the utility of using these techniques in the pharmacological characterization of novel drugs and propose the importance of information about pharmacokinetic properties. Translational PET research associated with PK/PD modeling and simulation in drug discovery and early clinical development would provide a sound basis for support of appropriate selection of candidate compound in preclinical stage and dose selection and optimization of dose regimens for early studies conducted in patients.

CNS disorders have a complex etiology and very few animal models are available to predict clinical efficacy. In this thesis, the contribution of target occupancy

to the pharmacological efficacy was well characterized by PK/PD analysis using PET.

This approach would also be used to the other CNS disorders if target molecule (e.g., receptor, transporter, enzyme) relevant to disease status. To avoid wasting time and resources, more reasonable and plausible approach would be required for future drug discovery. This imaging and modeling frameworks to develop a preclinical translation model could be applicable to other CNS drug discovery and development and contribute to improve productivity of pharmaceutical industries.

References

- 1) **Borsook D. Hargreaves R. Becerra L.**
Can Functional Magnetic Resonance Imaging Improve Success Rates in CNS Drug Discovery? *Expert Opin Drug Discov.* 2011;6(6):597-617.
- 2) **Hurko O. Ryan JL.**
Translational research in central nervous system drug discovery.
NeuroRx. 2005 ;2(4):671-82.
- 3) **Bonate PL.**
Editorial to the themed issue on translational modeling in neuroscience.
J Pharmacokinet Pharmacodyn. 2013;40(3):255
- 4) **Potter WZ.**
New era for novel CNS drug development.
Neuropsychopharmacology. 2012 ;37(1):278-80.
- 5) **O'Connell D. Roblin D.**
Translational research in the pharmaceutical industry: from bench to bedside.
Drug Discov Today. 2006;11(17-18):833-8.
- 6) **Gee AD.**
Neuropharmacology and drug development.
Br Med Bull. 2003;65:169-77.
- 7) **Koehler L. Gagnon K. McQuarrie S. Wuest F.**
Iodine-124: a promising positron emitter for organic PET chemistry.
Molecules. 2010;15(4):2686-718.
- 8) **Phelps ME.**
PET: the merging of biology and imaging into molecular imaging.
J Nucl Med. 2000 ;41(4):661-81.

9) **Phelps ME.**

Positron emission tomography provides molecular imaging of biological processes.

Proc Natl Acad Sci USA. 2000;97(16):9226-33.

10) **Paans AM. van Waarde A. Elsinga PH. Willemsen AT. Vaalburg W.**

Positron emission tomography: the conceptual idea using a multidisciplinary approach.

Methods. 2002;27(3):195-207.

11) **Hutchins GD. Miller MA. Soon VC. Receveur T.**

Small animal PET imaging.

ILAR J. 2008;49(1):54-65.

12) **Yang Y. Tai YC. Siegel S. Newport DF. Bai B. Li Q. Leahy RM. Cherry SR.**

Optimization and performance evaluation of the microPET II scanner for *in vivo* small-animal imaging.

Phys Med Biol. 2004;49(12):2527-45.

13) **Mager DE. Jusko WJ.**

Development of translational pharmacokinetic-pharmacodynamic models.

Clin Pharmacol Ther. 2008 ;83(6):909-12.

14) **Derendorf H. Lesko LJ. Chaikin P. Colburn WA. Lee P. Miller R. Powell R. Rhodes G. Stanski D. Venitz J.**

Pharmacokinetic/pharmacodynamic modeling in drug research and development.

J Clin Pharmacol. 2000;40(12 Pt 2):1399-418.

15) **Lesko LJ. Rowland M. Peck CC. Blaschke TF. Breimer D. de Jong HJ. Grahn A. Kuhlmann JJ. Stewart B.** Optimizing the science of drug development: opportunities for better candidate selection and accelerated evaluation in humans. *Eur J Pharm Sci.* 2000;10(4): iv-xiv.

16) Chien JY. Friedrich S. Heathman MA. de Alwis DP. Sinha V.

Pharmacokinetics/Pharmacodynamics and the stages of drug development: role of modeling and simulation. *AAPS J.* 2005;7(3):E544-59.

17) Workman P. Aboagye EO. Chung YL. Griffiths JR. Hart R. Leach MO. Maxwell RJ. McSheehy PM. Price PM. Zweit J.

Minimally invasive pharmacokinetic and pharmacodynamic technologies in hypothesis-testing clinical trials of innovative therapies.

J Natl Cancer Inst. 2006 ;98(9):580-98.

18) Cohen A.

Pharmacokinetic and pharmacodynamic data to be derived from early-phase drug development: designing informative human pharmacology studies.

Clin Pharmacokinet. 2008;47(6):373-81.

19) Thor KB. Katofiasc MA. Danuser H. Springer J. Schaus JM.

The role of 5-HT(1A) receptors in control of lower urinary tract function in cats.

Brain Res. 2002 Aug 16;946(2):290-7.

20) Chang HY. Cheng CL. Chen JJ. de Groat WC.

Roles of glutamatergic and serotonergic mechanisms in reflex control of the external urethral sphincter in urethane-anesthetized female rats.

Am J Physiol Regul Integr Comp Physiol. 2006;291(1):R224-34.

21) Ishizuka O. Gu B. Igawa Y. Nishizawa O. Pehrson R. Andersson KE.

Role of supraspinal serotonin receptors for micturition in normal conscious rats.

Neurourol Urodyn. 2002;21(3):225-30.

22) Khaled SM. Elhilali M.

Role of 5-HT receptors in treatment of overactive bladder.

Drugs Today (Barc). 2003;39(8):599-607.

23) Thor KB. Hisamitsu T. de Groat WC.

Unmasking of a neonatal somatovesical reflex in adult cats by the serotonin autoreceptor agonist 5-methoxy-N,N-dimethyltryptamine.

Brain Res Dev Brain Res. 1990;54(1):35-42.

24) Mittra S. Malhotra S. Naruganahalli KS. Chugh A.

Role of peripheral 5-HT_{1A} receptors in detrusor over activity associated with partial bladder outlet obstruction in female rats.

Eur J Pharmacol. 2007;561(1-3):189-93.

25) Kakizaki H. Yoshiyama M. Koyanagi T. De Groat WC.

Effects of WAY100635, a selective 5-HT_{1A}-receptor antagonist on the micturition-reflex pathway in the rat.

Am J Physiol Regul Integr Comp Physiol. 2001;280(5):R1407-13.

26) Abrams P. Cardozo L. Fall M. Griffiths D. Rosier P. Ulmsten U. Van Kerrebroeck P. Victor A. Wein A

The standardisation of terminology in lower urinary tract function: report from the standardisation sub-committee of the International Continence Society.

Urology. 2003;61(1):37-49.

27) Chapple CR. Khullar V. Gabriel Z. Muston D. Bitoun CE. Weinstein D.

The effects of antimuscarinic treatments in overactive bladder: an update of a systematic review and meta-analysis.

Eur Urol. 2008;54(3):543-62.

28) Kershen RT. Hsieh M.

Preview of new drugs for overactive bladder and incontinence: darifenacin, solifenacin, trospium, and duloxetine.

Curr Urol Rep. 2004 ;5(5):359-67.

29) **Scheife R. Takeda M.**

Central nervous system safety of anticholinergic drugs for the treatment of overactive bladder in the elderly.

Clin Ther. 2005;27(2):144-53.

30) **Cheng CL. de Groat WC.**

Role of 5-HT_{1A} receptors in control of lower urinary tract function in anesthetized rats.

Am J Physiol Renal Physiol. 2010;298(3):F771-8.

31) **Abanades S. van der Aart J. Barletta JA. Marzano C. Searle GE. Salinas CA. Ahmad JJ. Reiley RR. Pampols-Maso S. Zamuner S. Cunningham VJ. Rabiner EA. Laruelle MA. Gunn RN.**

Prediction of repeat-dose occupancy from single-dose data: characterisation of the relationship between plasma pharmacokinetics and brain target occupancy.

J Cereb Blood Flow Metab. 2011;31(3):944-52.

32) **McCarron JA. Turton DR. Pike VW. Poole KG**

Remotely-controlled production of the 5-HT_{1A} radioligand, [carbonyl-¹¹C]WAY-100635, via ¹¹C-carboxylation of an immobilized Grignard reagent.

J Label Compd Radiopharm. 1996; 38:941-953.

33) **Tai YC. Ruangma A. Rowland D. Siegel S. Newport DF. Chow PL. Laforest R.**

Performance evaluation of the microPET focus: a third-generation microPET scanner dedicated to animal imaging.

J Nucl Med. 2005;46(3):455-63.

34) **Lammertsma AA. Hume SP.**

Simplified reference tissue model for PET receptor studies.

Neuroimage. 1996;4(3 Pt 1):153-8.

35) **Andrée B. Hedman A. Thorberg SO. Nilsson D. Halldin C. Farde L.**

Positron emission tomographic analysis of dose-dependent NAD-299 binding to 5-hydroxytryptamine-1A receptors in the human brain.

Psychopharmacology (Berl). 2003;167(1):37-45.

36) **Rabiner EA. Wilkins MR. Turkheimer F. Gunn RN. Udo de Haes J. de Vries M. Grasby PM.**

5-Hydroxytryptamine 1A receptor occupancy by novel full antagonist 2-[4-[4-(7-chloro-2,3-dihydro-1,4-benzodioxyn-5-yl)-1-piperazinyl]butyl]-1,2-benzisothiazol-3-(2H)-one-1,1-dioxide: A [¹¹C][O-methyl-3H]-N-(2-(4-(2-methoxyphenyl)-1-piperazinyl)ethyl)-N-(2-pyridinyl)cyclohexanecarboxamide trihydrochloride (WAY-100635) positron emission tomography study in humans.

J Pharmacol Exp Ther. 2002;301(3):1144-50.

37) **Raje S. Patat AA. Parks V. Schechter L. Plotka A. Paul J. Langstrom B.**

A positron emission tomography study to assess binding of lecozotan, a novel 5-hydroxytryptamine-1A silent antagonist, to brain 5-HT_{1A} receptors in healthy young and elderly subjects, and in patients with Alzheimer's disease.

Clin Pharmacol Ther. 2008;83(1):86-96.

38) **Sheiner LB. Stanski DR. Vozeh S. Miller RD. Ham J.**

Simultaneous modeling of pharmacokinetics and pharmacodynamics: application to d-tubocurarine.

Clin Pharmacol Ther. 1979;25(3):358-71.

39) **Pehrson R. Ojteg G. Ishizuka O. Andersson KE.**

Effects of NAD-299, a new, highly selective 5-HT_{1A} receptor antagonist, on bladder function in rats.

Naunyn Schmiedebergs Arch Pharmacol. 2002 ;366(6):528-36.

40) **Saijo T. Maeda J. Okauchi T. Maeda J. Morio Y. Kuwahara Y. Suzuki M. Goto N. Fukumura T. Suhara T. Higuchi M.**

Presynaptic selectivity of a ligand for serotonin 1A receptors revealed by *in vivo* PET assays of rat brain. *PLoS One*. 2012;7(8):e42589.

41) **Kapur S. Seeman P.**

Antipsychotic agents differ in how fast they come off the dopamine D2 receptors. Implications for atypical antipsychotic action.

J Psychiatry Neurosci. 2000;25(2):161-6.

42) **Kato R. Yamazoe Y.**

Sex-specific cytochrome P450 as a cause of sex- and species-related differences in drug toxicity. *Toxicol Lett*. 1992;64-65:661-7.

43) **Chovan JP. Ring SC. Yu E. Baldino JP.**

Cytochrome P450 probe substrate metabolism kinetics in Sprague Dawley rats. *Xenobiotica*. 2007;37(5):459-73.

44) **Lecci A. Giuliani S. Santicoli P. Maggi CA.**

Involvement of 5-hydroxytryptamine_{1A} receptors in the modulation of micturition reflexes in the anesthetized rat.

J Pharmacol Exp Ther. 1992;262(1):181-9.

45) **Leonardi A. Testa R.**

Use of 5-HT_{1A} receptor antagonists for the treatment of urinary incontinence. *Application WO* 1997; 9731637-A1.

46) **Ramage AG.**

The role of central 5-hydroxytryptamine (5-HT, serotonin) receptors in the control of micturition.

Br J Pharmacol. 2006;147 Suppl 2:S120-31.

47) **Testa R. Guarneri L. Poggesi E. Angelico P. Velasco C. Ibba M. Cilia A. Motta G. Riva C. Leonardi A.**

Effect of several 5-hydroxytryptamine(1A) receptor ligands on the micturition reflex in rats: comparison with WAY 100635.

J Pharmacol Exp Ther. 1999;290(3):1258-69.

48) **de Groat WC.**

Integrative control of the lower urinary tract: preclinical perspective.

Br J Pharmacol. 2006;147 Suppl 2:S25-40.

49) **Maeda J. Suhara T. Kawabe K. Okauchi T. Obayashi S. Hojo J. Suzuki K.**

Visualization of alpha5 subunit of GABA_A/benzodiazepine receptor by [¹¹C]Ro15-4513 using positron emission tomography.

Synapse. 2003;47(3):200-8.

50) **Yamasaki T. Fujinaga M. Kawamura K. Yui J. Hatori A. Ohya T. Xie L. Wakizaka H. Yoshida Y. Fukumura T. Zhang MR.**

In vivo measurement of the affinity and density of metabotropic glutamate receptor subtype 1 in rat brain using ¹⁸F-FITM in small-animal PET.

J Nucl Med. 2012;53(10):1601-7.

51) **Olsson H. Halldin C. Farde L.**

Differentiation of extrastriatal dopamine D₂ receptor density and affinity in the human brain using PET.

Neuroimage. 2004;22(2):794-803.

52) **Farde L. Hall H. Ehrin E. Sedvall G.**

Quantitative analysis of D₂ dopamine receptor binding in the living human brain by PET.

Science. 1986;231(4735):258-61.

53) Farde L. Eriksson L. Blomquist G. Halldin C.

Kinetic analysis of central [¹¹C]raclopride binding to D₂-dopamine receptors studied by PET : A comparison to the equilibrium analysis.

J Cereb Blood Flow Metab. 1989;9(5):696-708.

54) Ito H. Hietala J. Blomqvist G. Halldin C. Farde L.

Comparison of the transient equilibrium and continuous infusion method for quantitative PET analysis of [¹¹C]raclopride binding.

J Cereb Blood Flow Metab. 1998;18(9):941-50.

55) Olsson H. Farde L.

Potentials and pitfalls using high affinity radioligands in PET and SPET determinations on regional drug induced D₂ receptor occupancy: A simulation study based on experimental data.

Neuroimage. 2001;14(4):936-45.

56) Olsson H. Halldin C. Swahn CG. Farde L.

Quantification of [¹¹C]FLB 457 binding to extrastriatal dopamine receptors in the human brain. *J Cereb Blood Flow Metab.* 1999;19(10):1164-73.

57) Onoe H. Tsukada H. Nishiyama S. Nakanishi S. Inoue O. Långström B. Watanabe Y.

A subclass of GABA_A/benzodiazepine receptor exclusively localized in the limbic system.

Neuroreport. 1996;8(1):117-22.

58) Okauchi T. Suhara T. Maeda J. Kawabe K. Obayashi S. Suzuki K.

Effect of endogenous dopamine on endogenous dopamine on extrastriated [¹¹C]FLB 457 binding measured by PET.

Synapse. 2001;41(2):87-95.

59) **Farde L. Pauli S. Hall H. Eriksson L. Halldin C. Högberg T. Nilsson L. Sjögren**

I. Stone-Elander S.

Stereoselective binding of [¹¹C]raclopride in living human brain : A search for extrastriatal central D2-dopamine receptors by PET.

Psychopharmacology (Berl). 1988 94(4):471-8.

60) **Lanfumey L. Hamon M.**

Central 5-HT_{1A} receptors: regional distribution and functional characteristics.

Nucl Med Biol. 2000;27(5):429-35.

61) **Pardridge WM.**

Blood-brain barrier delivery.

Drug Discov Today. 2007;12(1-2):54-61.

62) **Taylor EM.**

The impact of efflux transporters in the brain on the development of drugs for CNS disorders. *Clin Pharmacokinet*. 2002; 41(2):81-92.

63) **Elsinga PH. Hendrikse NH. Bart J. van Waarde A. Vaalburg W.F**

Positron emission tomography studies on binding of central nervous system drugs and P-glycoprotein function in the rodent brain.

Mol Imaging Biol. 2005;7(1):37-44.

64) **Elsinga PH. Hendrikse NH. Bart J. Vaalburg W. van Waarde A.**

PET Studies on P-glycoprotein function in the blood-brain barrier: how it affects uptake and binding of drugs within the CNS.

Curr Pharm Des. 2004;10(13):1493-503.

65) **Pike VW.**

PET radiotracers: crossing the blood-brain barrier and surviving metabolism.

Trends Pharmacol Sci. 2009;30(8):431-40.

66) **Ishiwata K. Kawamura K. Yanai K. Hendrikse NH.**

In vivo evaluation of P-glycoprotein modulation of 8 PET radioligands used clinically. *J Nucl Med.* 2007;48(1):81-7.

67) **Kuntner C. Bankstahl JP. Bankstahl M. Stanek J. Wanek T. Stundner G. Karch R. Brauner R. Meier M. Ding X. Müller M. Löscher W. Langer O.**

Dose-response assessment of tariquidar and elacridar and regional quantification of P-glycoprotein inhibition at the rat blood-brain barrier using (R)-[¹¹C]verapamil PET. *Eur J Nucl Med Mol Imaging.* 2010;37(5):942-53.

68) **Bankstahl JP. Kuntner C. Abraham A. Karch R. Stanek J. Wanek T. Wadsak W. Kletter K. Müller M. Löscher W. Langer O.**

Tariquidar-induced P-glycoprotein inhibition at the rat blood-brain barrier studied with (R)-¹¹C-verapamil and PET. *J Nucl Med.* 2008;49(8):1328-35.

69) **Witherspoon SM. Emerson DL. Kerr BM. Lloyd TL. Dalton WS. Wissel PS.**

Flow cytometric assay of modulation of P-glycoprotein function in whole blood by the multidrug resistance inhibitor GG918. *Clin Cancer Res.* 1996;2(1):7-12.

70) **Allen JD. Brinkhuis RF. Wijnholds J. Schinkel AH.**

The mouse Bcrp1/Mxr/Abcp gene: amplification and overexpression in cell lines selected for resistance to topotecan, mitoxantrone, or doxorubicin. *Cancer Res.* 1999;59(17):4237-41.

71) **Martin C. Berridge G. Mistry P. Higgins C. Charlton P. Callaghan R.**

The molecular interaction of the high affinity reversal agent XR9576 with P-glycoprotein. *Br J Pharmacol.* 1999;128(2):403-11.

- 72) **Choo EF. Kurnik D. Muszkat M. Ohkubo T. Shay SD. Higginbotham JN. Glaeser H. Kim RB. Wood AJ. Wilkinson GR.**
Differential *in vivo* sensitivity to inhibition of P-glycoprotein located in lymphocytes, testes, and the blood-brain barrier.
J Pharmacol Exp Ther. 2006;317(3):1012-8.
- 73) **Cutler L. Howes C. Deeks NJ. Buck TL. Jeffrey P.**
Development of a P-glycoprotein knockout model in rodents to define species differences in its functional effect at the blood-brain barrier.
J Pharm Sci. 2006;95(9):1944-53.
- 74) **Bihorel S. Camenisch G. Lemaire M. Scherrmann JM.**
Influence of breast cancer resistance protein (Abcg2) and p-glycoprotein (Abcb1a) on the transport of imatinib mesylate (Gleevec) across the mouse blood-brain barrier.
J Neurochem. 2007;102(6):1749-57.
- 75) **Chen Y. Agarwal S. Shaik NM. Chen C. Yang Z. Elmquist WF.**
P-glycoprotein and breast cancer resistance protein influence brain distribution of dasatinib. *J Pharmacol Exp Ther.* 2009;330(3):956-63.
- 76) **Lagas JS. van Waterschoot RA. van Tilburg VA. Hillebrand MJ. Lankheet N. Rosing H. Beijnen JH. Schinkel AH.**
Brain accumulation of dasatinib is restricted by P-glycoprotein (ABCB1) and breast cancer resistance protein (ABCG2) and can be enhanced by elacridar treatment.
Clin Cancer Res. 2009;15(7):2344-51.
- 77) **Agarwal S. Sane R. Gallardo JL. Ohlfest JR. Elmquist WF.**
Distribution of gefitinib to the brain is limited by P-glycoprotein (ABCB1) and breast cancer resistance protein (ABCG2)-mediated active efflux.
J Pharmacol Exp Ther. 2010;334(1):147-55.

78) **Tang SC. Lagas JS. Lankheet NA. Poller B. Hillebrand MJ. Rosing H. Beijnen JH. Schinkel AH.**

Brain accumulation of sunitinib is restricted by P-glycoprotein (ABCB1) and breast cancer resistance protein (ABCG2) and can be enhanced by oral elacridar and sunitinib coadministration.

Int J Cancer. 2012;130(1):223-33.

79) **Lagas JS. van Waterschoot RA. Sparidans RW. Wagenaar E. Beijnen JH. Schinkel AH.**

Breast cancer resistance protein and P-glycoprotein limit sorafenib brain accumulation.

Mol Cancer Ther. 2010;9(2):319-26.

80) **Laćan G. Plenevaux A. Rubins DJ. Way BM. Defraiteur C. Lemaire C. Aerts J. Luxen A. Cherry SR. Melega WP.**

Cyclosporine, a P-glycoprotein modulator, increases [¹⁸F]MPPF uptake in rat brain and peripheral tissues: microPET and ex vivo studies.

Eur J Nucl Med Mol Imaging. 2008;35(12):2256-66.

81) **Marcinkiewicz M. Vergé D. Gozlan H. Pichat L. Hamon M.**

Autoradiographic evidence for the heterogeneity of 5-HT₁ sites in the rat brain.

Brain Res. 1984;291(1):159-63.

82) **Plenevaux A. Weissmann D. Aerts J. Lemaire C. Brihaye C. Degueldre C. Le Bars D. Comar D. Pujol J. Luxen A.**

Tissue distribution, autoradiography, and metabolism of 4-(2'-methoxyphenyl)-1-[2'-[N-2"-pyridinyl)-p-[¹⁸F]fluorobenzamido]ethyl]piperazine (p-[¹⁸F]MPPF), a new serotonin 5-HT_{1A} antagonist for positron emission tomography: An *In vivo* study in rats.

J Neurochem. 2000 Aug;75(2):803-11.

83) USFDA.

Challenge and Opportunity on the Critical Path to New Medical Products.

<http://www.fda.gov/ScienceResearch/SpecialTopics/CriticalPathInitiative/CriticalPathOpportunitiesReports/ucm077262.htm> 2004

84) Grimwood S. Hartig PR.

Target site occupancy: emerging generalizations from clinical and preclinical studies.

Pharmacol Ther. 2009 Jun;122(3):281-301.

85) Fox GB. Chin CL. Luo F. Day M. Cox BF.

Translational neuroimaging of the CNS: novel pathways to drug development.

Mol Interv. 2009;9(6):302-13.

86) Wong DF. Tauscher J. Gründer G.

The role of imaging in proof of concept for CNS drug discovery and development.

Neuropsychopharmacology. 2009;34(1):187-203.

87) Lee CM. Farde L.

Using positron emission tomography to facilitate CNS drug development.

Trends Pharmacol Sci. 2006 Jun;27(6):310-6.

88) de Groat WC.

Influence of central serotonergic mechanisms on lower urinary tract function.

Urology. 2002 May;59(5 Suppl 1):30-6.

Figures

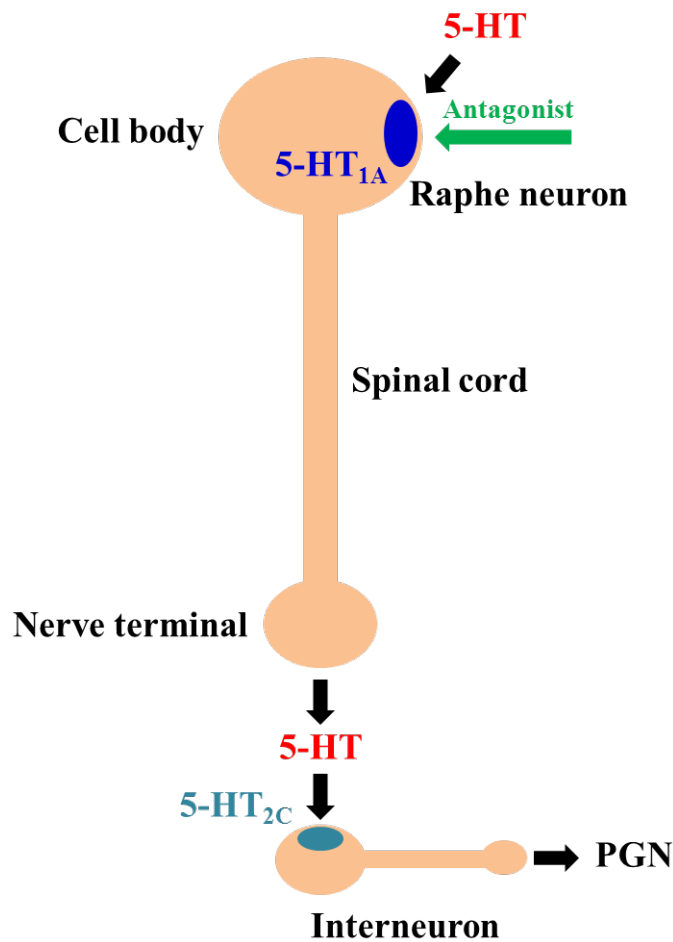
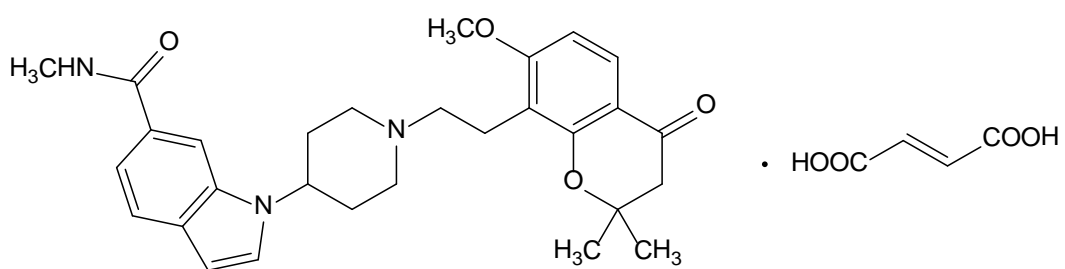


Figure 1 Serotonergic pathways controlling bladder functions in the rat. Descending projections from the brainstem raphe neurons to the spinal cord activate segmental interneurons that provide an inhibitory input to the parasympathetic preganglionic neurons (PGN) innervating the bladder. Blockade of inhibitory 5-HT_{1A} autoreceptors in the raphe neurons enhances raphe neuron firing and, increases the release of 5-HT in the spinal cord. 5-HT activates excitatory 5-HT_{2C} receptors on inhibitory interneurons, which then suppresses PGN firing^[88].



Chemical name:

1-{1-[2-(7-Methoxy-2,2-dimethyl-4-oxochroman-8-yl)ethyl]piperidin-4-yl}-*N*-methyl-1*H*-indole-6-carboxamide fumarate

Molecular formula: $C_{29}H_{35}N_3O_4 \cdot C_4H_4O_4$ ($C_{33}H_{39}N_3O_8$)

Molecular weight: 605.68 (489.62 as free form)

Figure 2 Chemical structure of E2110

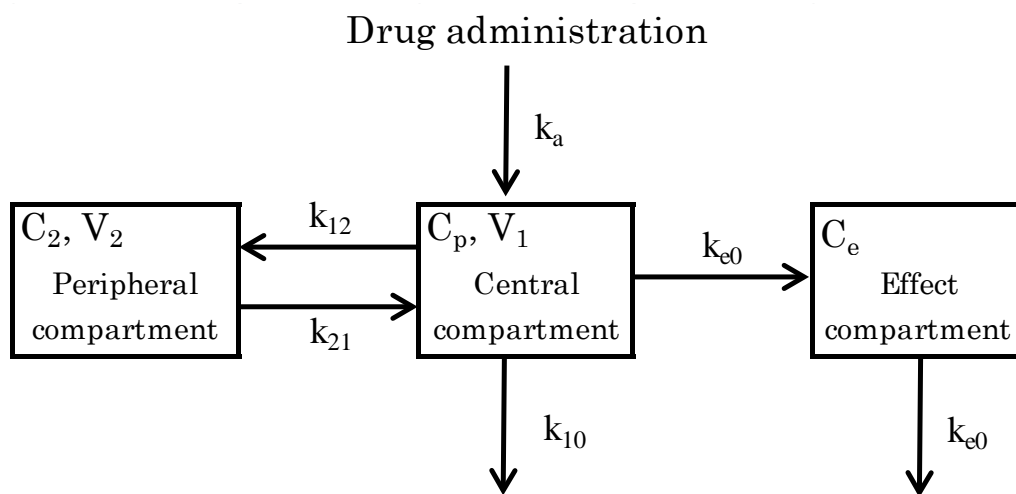


Figure 3 Schematic illustration of a model for description of E2110 PK/PD. C_p , E2110 concentration in the central compartment; C_e , E2110 concentration in the effect compartment; k_a , absorption rate constant; k_{e0} , equilibrium rate constant; V_1 , central volume of distribution; V_2 , peripheral volume of distribution

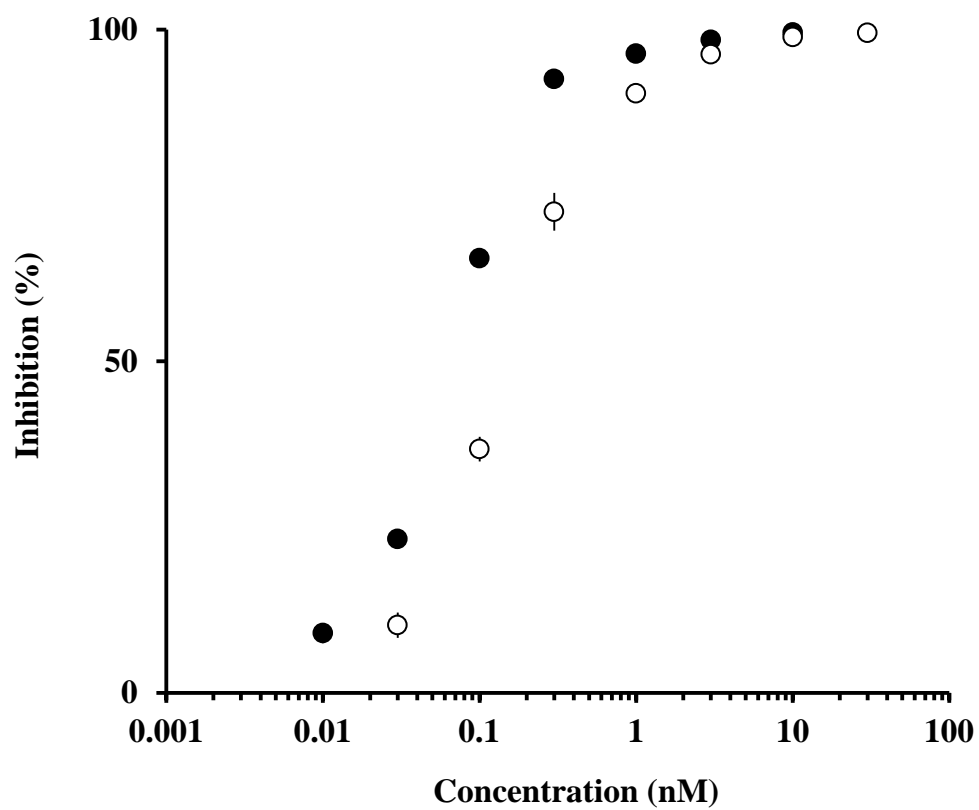


Figure 4 *In vitro* inhibition profiles of E2110 and WAY-100635 on 5-HT_{1A} receptors. Inhibition of specific [³H]MPPF binding in rat hippocampal membrane homogenates was measured at various concentrations of E2110 (●) and WAY-100635 (○)

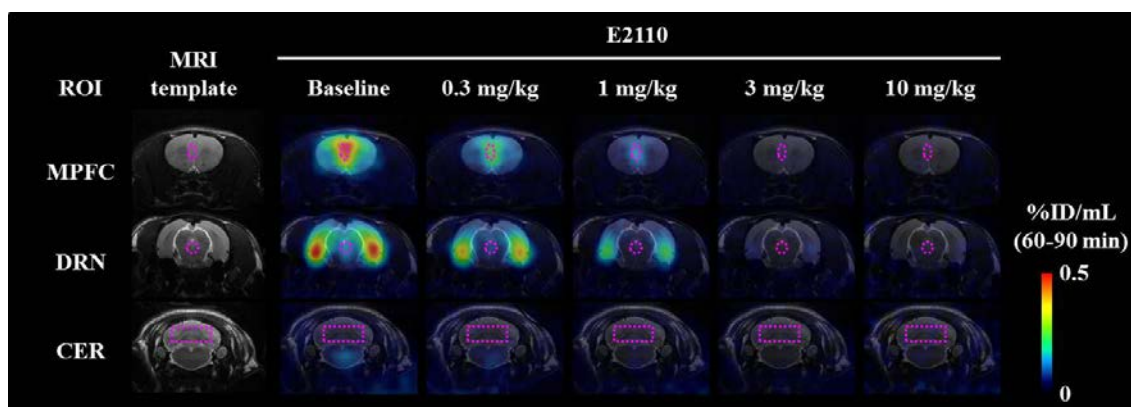


Figure 5 Representative PET images illustrating distribution of [^{11}C]WAY-100635 in rat brains at baseline and after oral administration of E2110. PET images were generated by averaging dynamic data at 60–90 min after intravenous radiotracer injection, and were overlaid on the MRI template shown in the far left column. Coronal brain sections shown here were obtained at 1.0 mm (top row), -7.8 mm (middle row) and -12.5 mm (bottom row) from the bregma. ROIs (dotted lines) were defined on the MPFC (top row), DRN (middle row) and cerebellum (CER; bottom row). The radiotracer retention was presented as a percentage of the injected dose per unit tissue volume (%ID/mL)

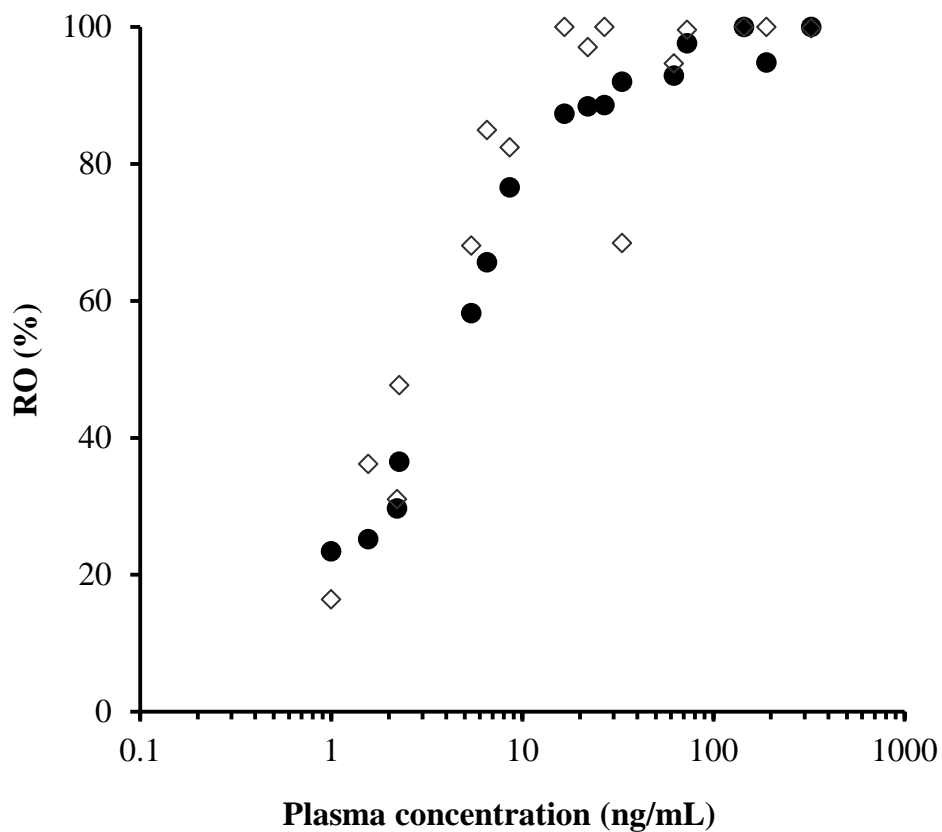


Figure 6 Relationship between rat 5-HT_{1A} RO (MPFC: ●, DRN: ◇) and E2110 plasma concentration. 5-HT_{1A} RO was determined at 4 hours after oral administration of E2110 at a dose ranging from 0.3 to 10 mg/kg. Symbols represent individual data from all dose levels (n = 4/dose level).

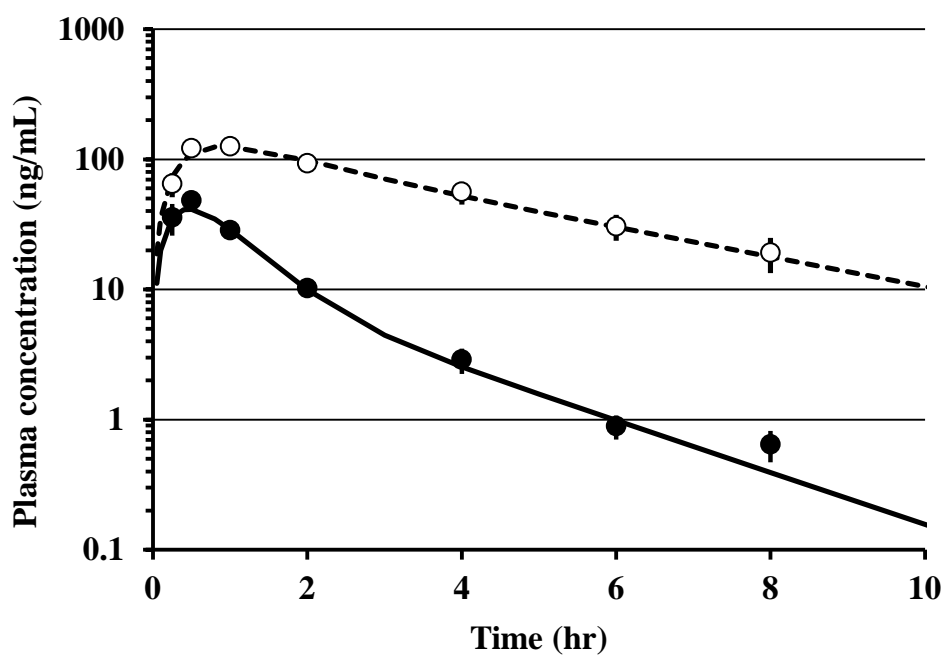


Figure 7 Plasma PK profile of E2110 after oral administration to rats. Symbols denote observed plasma concentrations (mean \pm S.E.M, n = 4/time point) in male (●) and female SD rats (○). Lines represent fitting of a two-compartment PK model with first-order absorption to the experimental data

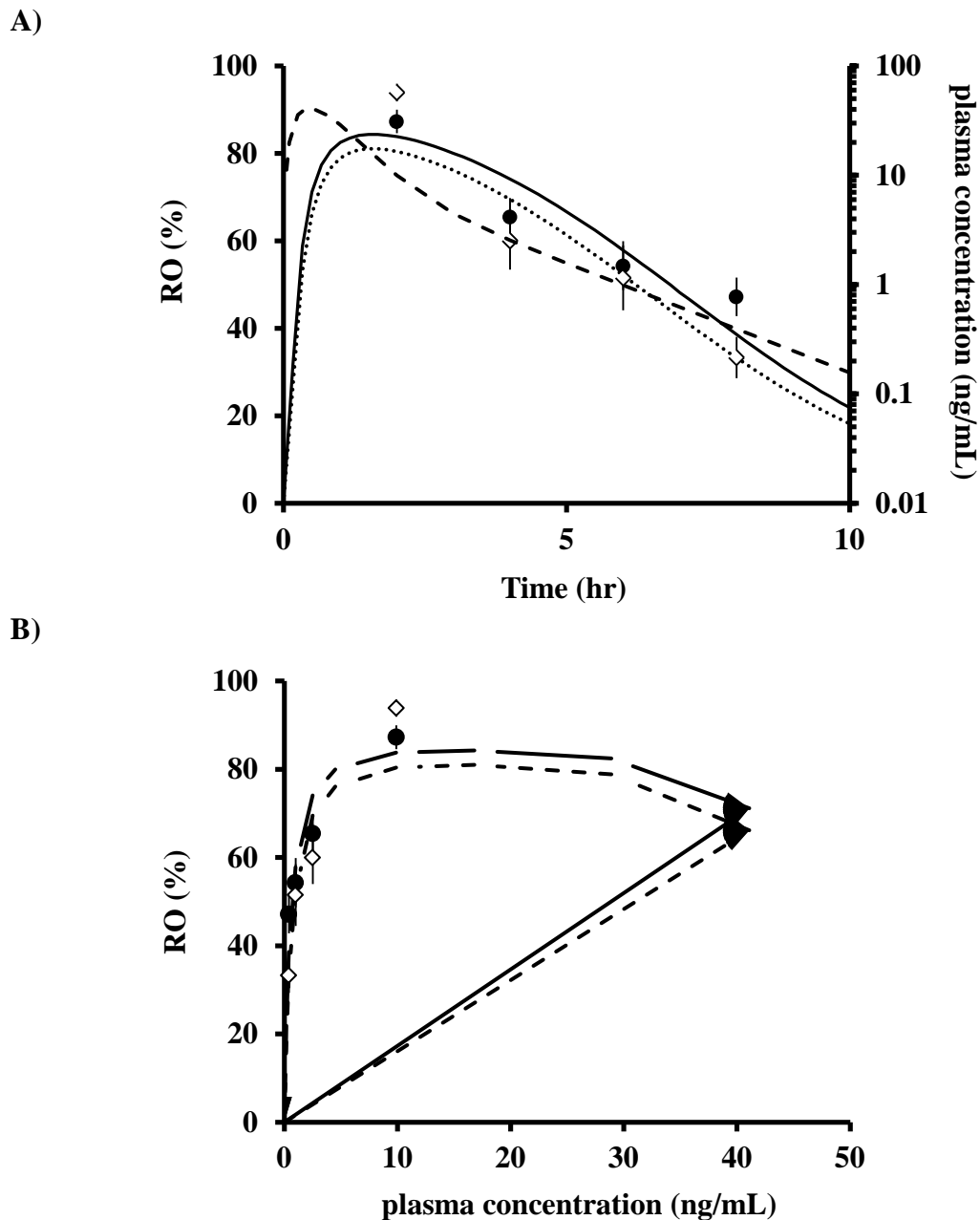


Figure 8 Time course data of rat 5-HT_{1A} RO in MPFC (●) and DRN (◇), and plasma E2110 concentration (thick dashed line) (A), and plot of RO against plasma E2110 concentration at individual time points (B). 5-HT_{1A} RO was determined at assigned time points after oral administration of E2110 at a dose of 1 mg/kg. Symbols represent mean \pm S.E.M at indicated time points (n = 4/time point). Lines indicate the predicted occupancy versus plasma concentration in MPFC (solid line) and DRN (dashed line)

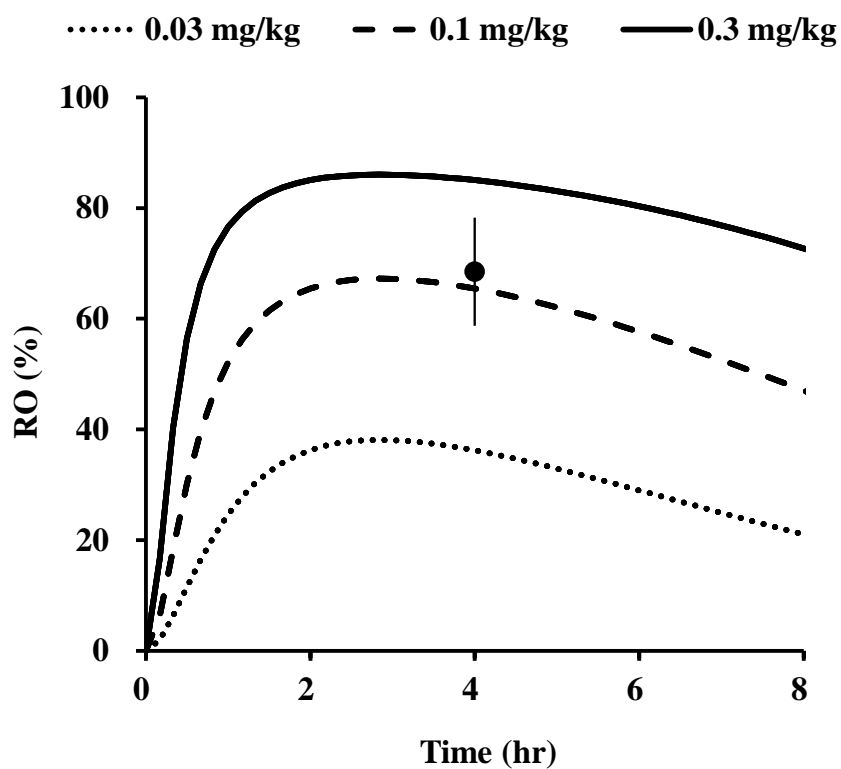


Figure 9 Effect compartment model estimation of 5-HT_{1A} RO in DRN after oral administration of E2110 at doses of 0.03, 0.1 and 0.3 mg/kg to female rats. Solid circle and error bars represent mean RO \pm S.E.M measured by PET scans in female rats (n = 3).

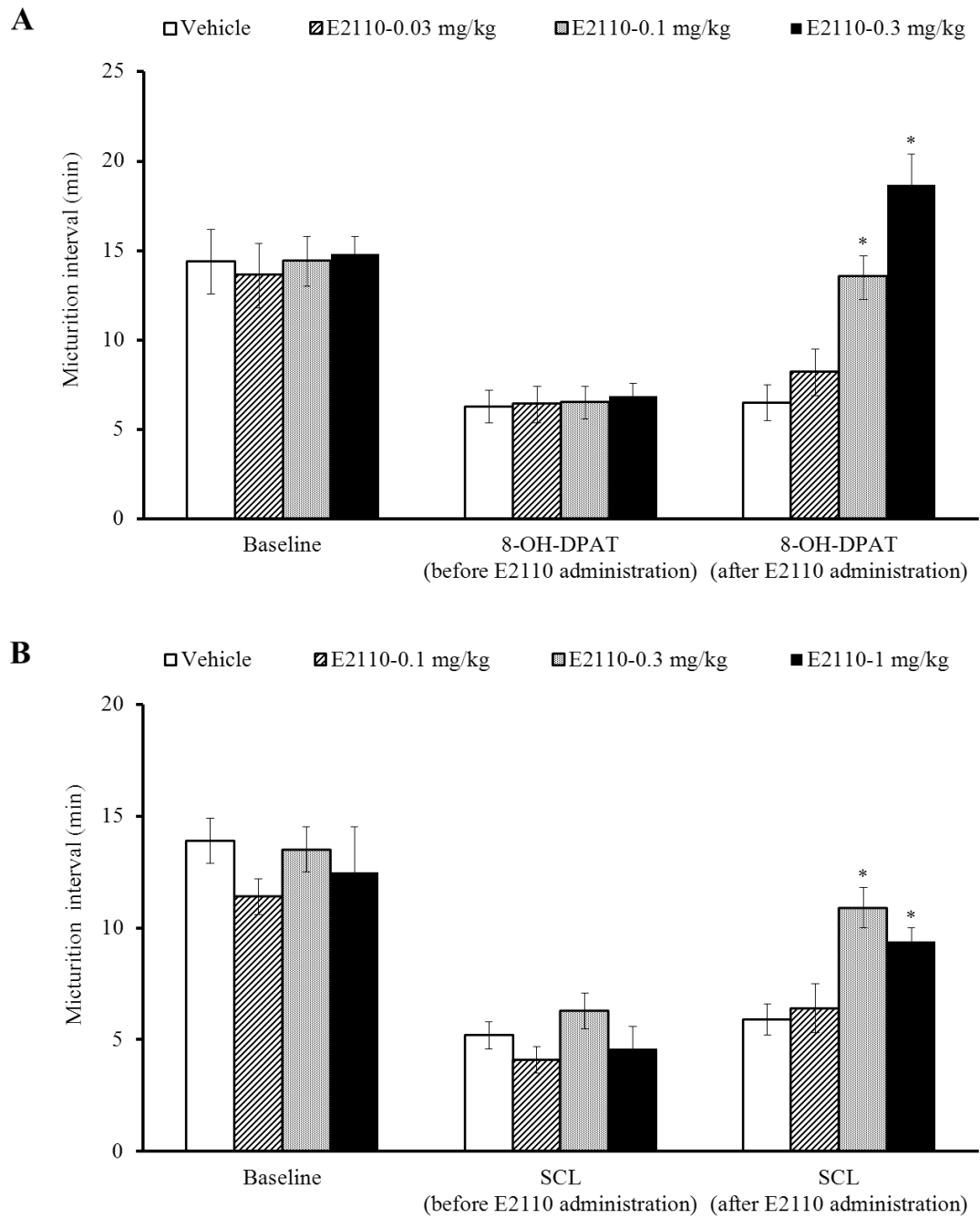


Figure 10 Effects of E2110 on micturition interval in 8-OH-DPAT-infused (A) and SCL (B) rats. Values are expressed as mean \pm S.E.M. of eight rats in 8-OH-DPAT-infused and SCL models; * $P < 0.05$ versus vehicle (Dunnett's multiple test)

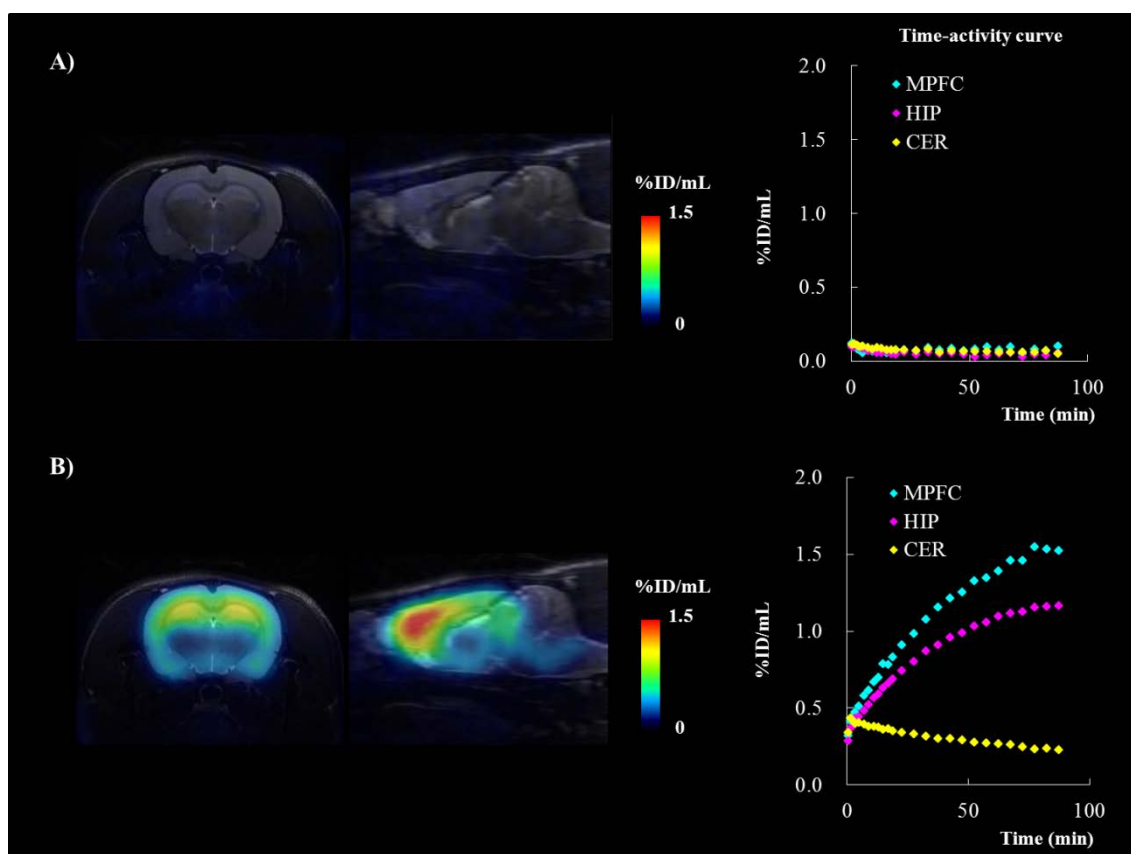


Figure 11 Representative PET images illustrating distribution of [^{11}C]E2110 and time-activity curve in rat brains at baseline (A) and 3 mg/kg of elacridar treatment conditions (B). PET images were generated by averaging dynamic data at 0–90 min after intravenous radiotracer injection, and were overlaid on the MRI template. ROIs were defined on the MPFC, HIP and CER (as reference region). The radiotracer retention was presented as a percentage of the injected dose per unit tissue volume (%ID/mL)

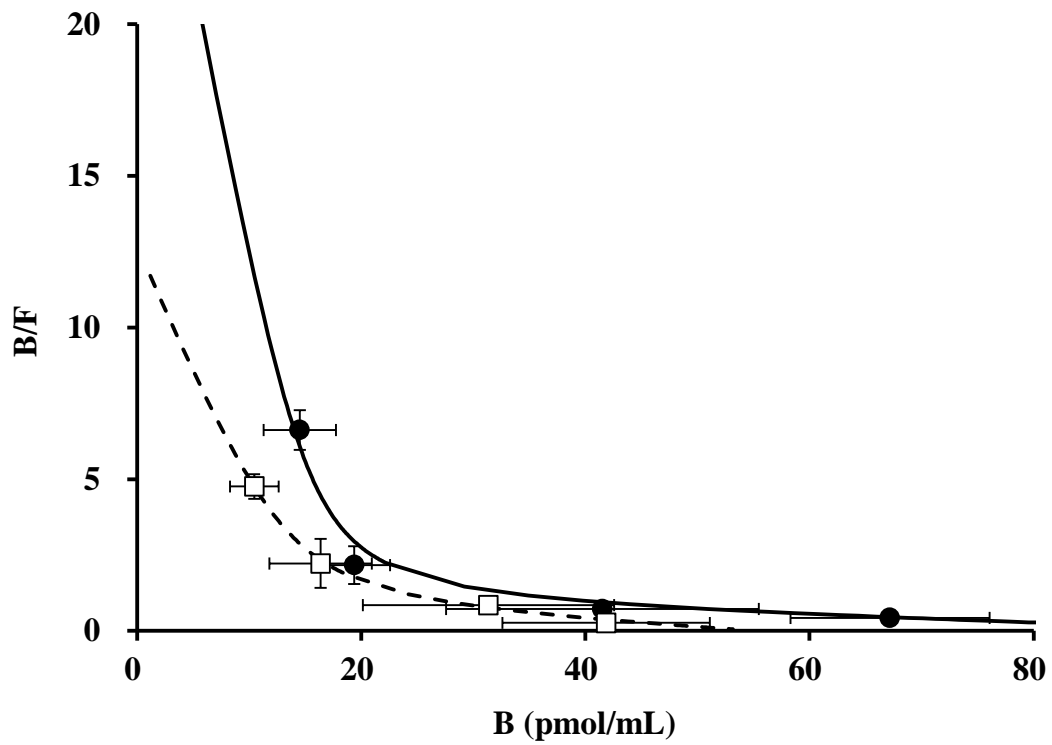


Figure 12 Scatchard plot of [^{11}C]E2110 specific binding in MPFC (●) and HIP (□). The continuous and broken lines show the regression lines for each region by two-site binding model.

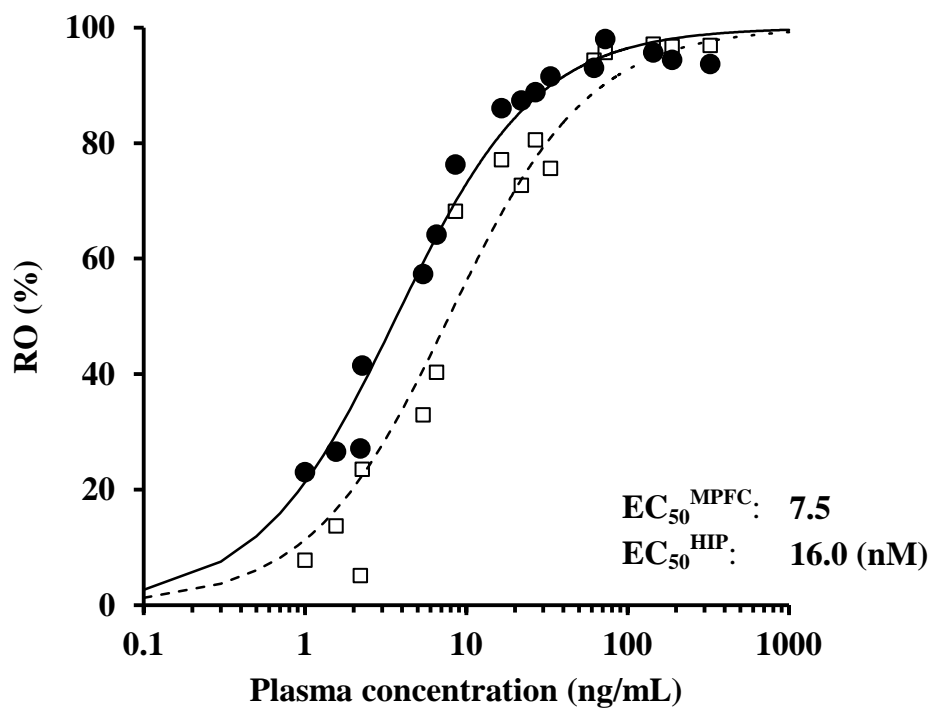


Figure 13 Relationship between rat 5-HT_{1A} RO (MPFC: ●, HIP: □) and E2110 plasma concentration. The continuous and broken lines show the regression lines for each region. Symbols represent individual data from all dose levels (see Chapter 1).

Tables

Table 1 *In vitro* pharmacological profile and *in vivo* PD parameter estimates for E2110.

<i>In vitro</i>		<i>In vivo</i>			
5-HT _{1A} receptor affinity		ROI		Dose-response study	Time-course study
K _i (nM)	0.045	EC ₅₀ (nM)	MPFC	7.51 (0.45 [*])	5.85 (0.35 [*])
			DRN	5.40 (0.32 [*])	7.38 (0.44 [*])

*: free concentration based value.

Table 2 PK parameter estimates after oral administration of E2110 to male and female SD rats.

Pharmacokinetic parameters	Male	Female
t _{1/2} (hr)	1.5	2.6
C _{max} (µg/mL)	48.1	125.7
T _{max} (hr)	0.5	1
AUC _{0-8hr} (µg•hr/mL)	71.8	487.9

Table 3 *In vivo* measurements of K_d, B_{max}, and BP by Scatchard analysis in rat brain.

Region	<i>High Affinity</i>			<i>Low Affinity</i>			R ^{2‡}
	K _{d1}	B _{max1}	BP ₁ [†]	K _{d2}	B _{max2}	BP ₂ [†]	
MPFC	0.5	15.1	30.3	101.4	87.8	0.9	0.82
HIP	1.1	13.1	11.9	51.5	42.1	0.8	0.87

Unit: K_d (nM), B_{max} (pmol/mL)

†: BP = B_{max}/K_d

‡: Coefficient of determination.

Acknowledgements

This work was carried at Department of Molecular Neuroimaging, National Institute of Radiological Sciences (NIRS) as a Cooperation Program Graduate Student, Molecular Imaging Educational/Training Course, Collaborative Chairs of Tohoku University School of Medicine.

I would like to express my sincere gratitude to:

Prof. Tetsuya Suhara (Head of Department of Molecular Neuroimaging), for his generous support as an organizer, for guidance and for numerous suggestions.

Assoc. Prof. Makoto Higuchi (Department of Molecular Neuroimaging), for his generous support of all experiments and manuscripts, and for his supportive advices and continuous encouragement during whole of my work as supervisor.

Prof. Kazuhiro Yanai (Department of Pharmacology, Tohoku University Graduate School of Medicine), for his sincere intermediation between NIRS and Tohoku University about Molecular Imaging Educational/Training Course.

Prof. Hiroo Matsuoka (Department of Psychiatry, Tohoku University Graduate School of Medicine), **Assoc. Prof. Nobuyuki Okamura** (Department of Pharmacology, Tohoku University Graduate School of Medicine), and **Prof. Manabu Tashiro** (Division of Cyclotron nuclear Medicine, Cyclotron and Radioisotope Center, Tohoku University), for their rigorous and courteous judgment for this thesis.

Dr. Jun Maeda, Dr. Masaki Tokunaga, Mr. Takeharu Minamihisamatsu (Molecular Neuroimaging Group, Molecular Center, NIRS), and **Mr. Takashi Okauchi** (Molecular Probe Dynamics Laboratory, RIKEN Center for Molecular Imaging Science), for their generous supports of animal experiments and PET system operations.

The staff at the Cyclotron Unit and Molecular Probe Group (Molecular Imaging Center, NIRS), for their precise cyclotron operation for production of radioisotopes and synthesis of [^{11}C]WAY100635.

Dr. Tsutomu Yoshimura, Dr. Kazutomi Kusano, and Dr. Osamu Takenaka, (DMPK Tsukuba Research Laboratory, Eisai Co., Ltd), for giving me the opportunity to do my PhD through the collaborative research with NIRS.

Dr. Norihito Oi (Biomarker Research Unit, Tsukuba Research Laboratory, Eisai Co., Ltd), for his great skill in chemistry and reliable supply of radiolabeled E2110.

Dr. Michiyuki Suzuki (Neuroscience Research Unit, Tsukuba Research Laboratory, Eisai Co., Ltd), for his generous support of animal experiment and suggestions from the pharmacologist's point of view.

Mr. Takashi Yoshinaga, Mrs. Miyuki Sakai, Mr. Hiroki Ishihara, and all members involved in the discovery and development of E2110 (Eisai Co., Ltd), for their kind advices on the pharmacology of E2110.

All my colleagues at the Molecular Neuroimaging Group (NIRS), and at the DMPK Department (Tsukuba Research Laboratory, Eisai Co., Ltd), for their help and creating a pleasant working atmosphere.

Greatest thanks of all go to my wife **Ayumi**. She supported me in every possible way and helped me keep my life in proper perspective and balance. This dissertation is dedicated to her with my deepest love, respect, and gratitude.